IMPROVEMENT OF THE PERFORMANCE OF A COKE DRUM OPERATION USING A COMPUTATIONAL FLUID DYNAMIC PERSPECTIVE

Amérika Yihan Arévalo Mosquera
Chemical Engineer

Universidad Nacional de Colombia
Facultad de Minas
Departamento de Procesos y Energía
Medellín, Colombia
July 2017

IMPROVEMENT OF THE PERFORMANCE OF A COKE DRUM OPERATION USING A COMPUTATIONAL FLUID DYNAMIC PERSPECTIVE

Amérika Yihan Arévalo Mosquera
Chemical Engineer

Thesis work presented as partial requirement for the degree of
Master of Engineering - Chemical Engineering

Advisor
Alejandro Molina Ochoa
Doctor of Engineering

Universidad Nacional de Colombia
Facultad de Minas
Departamento de Procesos y Energía
Medellín, Colombia
July 2017

To Garabata & Rasputin

Acknowledgments

Quiero agradecer en primer lugar al Instituto Colombiano del Petróleo (ICP-Ecopetrol) por la financiación del proyecto "Desarrollo de herramientas de simulación para la refinación de crudos pesados − Aproximación mediante dinámica de fluidos computacional (CFD)".

A mi tutor, Alejandro Molina por su guía y por brindarme la oportunidad de pertenecer al grupo de investigación Bioprocesos y Flujos Reactivos (Bio−frun). Agradezco todo su apoyo académico en el desarrollo de esta tesis.

Debo agradecer también a mis compañeros de proyecto por sus aportes que fueron muy significativos en el desarrollo de esta tesis. Particularmente debo agradecer a David Soto por todo su apoyo con respecto al manejo de la herramienta de simulación Ansys-Fluent y por estar ahí siempre que lo he necesitado al respecto.

Habiendo finalizado los agradecimientos académicos, prosigo a mencionar a los agradecimientos personales hacia quienes han estado apoyándome sin importar las adversidades del camino.

Primero quiero agradecer a mi familia, particularmente a la persona que ha estado a lo largo de mi vida apoyándome, brindándome consejos, regañándome cuando ha sido necesario e incluyéndome en sus oraciones: mi mami o Doña mami, como la llaman algunos de mis amigos.

Le doy un agradecimiento muy especial a persona que me ha acompañado por más de once años, que me ha brindado consejo, me ha apoyado en todos mis proyectos, que me conoce mejor que yo misma y ha estado acompañándome, así sea a distancia, en los momentos que lo he necesitado; a mi amigato Daniel Morillo.

En los momentos difíciles es cuando una persona sabe quiénes son esas personas que están a su lado y las puedes llamar "amigos". Los que más se han preocupado por mí en momentos de enfermedad, dificultades económicas y, porque no, en consejo y apoyo moral. Entre ellos están: Sandra, Yul, Diego (Cachorro), Pola, JuanFe, Armando y Betty.

También agradezco a mi pareja, Andrés Sánchez, quien ha estado conmigo a pesar de las dificultades que he pasado, por escucharme cuando lo he necesitado, por recordarme cosas que ya sé, pero a veces no las tengo en cuenta; por acompañarme a mis citas médicas, por más traumáticas que fueran.

A mi médico de confianza, a quién he podido consultar siempre que lo he necesitado, de quien he tenido muy buenas recomendaciones y por no juzgarme.

A mi psicóloga Rosa Correa, que se ha preocupado por mí y que incluso en momentos de dificultad económica ha estado ahí.

Finalmente debo agradecer a mis demonios, gracias a ellos cada vez soy una mujer más fuerte.

Abstract

The delayed coking process is used in petrochemical industry for upgrading heavy crude oils such as residues from vacuum towers or Vacuum Residue Crude (VRC) and atmospheric bottoms. A delayed coking unit has three main parts: a fractionation tower, a furnace and a coke drum (reactor) in which the residue is converted into valuable products. The coke drum operates like an adiabatic semi-batch reactor and thermal cracking reactions are carried out inside the reactor.

The coke drum is the main part of the process, it is important to identify possible bottlenecks and improve the performance of the coke drum operation. The selection of the main bottlenecks was carried out taking into account the most relevant process reported in industry. The source of that information could be: surveys in which representatives from some refineries discuss relevant issues and problems related to the coke drum, gray literature that describes operational problems in the delayed coking process and academic literature with a description of some problems of the delayed coking process, mainly for the coke drum.

According to literature review, one of the most important bottlenecks is the plug of the vapor line. The possible routes for coke formation are condensation of high boiling point components, chemical reaction and mechanical deposition of coke. The three routes were evaluated and according to this, it was determined that there is not coke formation by condensation or chemical reaction.To evaluate the coke formation because of particles and drops shift, a CFD simulation was carried out. For CFD simulation it is important to know some physical properties of the compounds. To obtain this properties a simulation was carried out using the Delayed Coker Model from Aspen Hysys.

A possible coke formation in the vapor line because of drops shift was obtained as result of the CFD simulation. To avoid the coke formation because of drops shift for a base case (tube at level with the reactor's surface), a modification of vapor line was proposed. This modification consists in introduce a section of vapor line into the reactor. To define the relevance of this modification, two cases were evaluated: the introduction of the vapor line 30 cm and 3 m. According to these modifications, the introduction of the tube implies a reduction of the coke deposition. However, there is not a significant diference between the first case (30 cm) and the second one (3 m).

To trying improve the above mentioned results, a geometry modification was proposed. It consists in modify the diameter of the coke drum at the top to increase the cross area and reduce the particle velocity which it is possible to delay the deposition of the particles. However, this alternative does not improve the previous results, by contrast, the coke deposition increased for the new geometry.

Resumen

El proceso de coquización lenta es usado en la industria petroquímica con el fin de refinar crudos pesados tales como residuos provenientes de las torres de vacío (VRC) y los fondos de las torres atmosféricas.

Una unidad de coquización lenta consta de tres partes principalmente: una torre fraccionadora, un horno de precalentamiento y un par de reactores (drums) en los cuales el residuo se convierte en productos más livianos. Los drums operan como reactores semi-batch donde se llevan a cabo reacciones de craqueo.

El drum es la parte más importante de este proceso, por tanto, es importante identificar posibles "cuellos de botella" y mejorar el rendimiento de la operación del drum. Los posibles "cuellos de botella" la evaluación de los posibles cuellos de botella se realizó teniendo en cuenta los problemas más relevantes reportados en la industria petroquímica. La fuente de dicha información fue tomada de encuestas, en las cuales representantes de algunas refinerías discuten sobre cuestiones relevantes y problemas relacionadas con el proceso; "literatura gris" en la cual se describen algunos problemas en la operación del proceso en cuestión y literatura académica con la descripción de algunos problemas del proceso de coquización lenta, principalmente en los drums.

De acuerdo con la revisión de literature, uno de los principales "cuellos de botella" es el taponamiento de la linea de vapor debido a la formación de coque. Las posibles rutas para la formación de coque son: condensación de componentes con alto punto de ebullición, formación de coque por reacción química y la deposición mecánica de partículas semicoquizadas. Las tres rutas fueron evaluadas y se obtuvo que para los casos de condensación y de reaccón química no hay producción de coque. Para evaluar la formación de coque debido al arrastre de gotas y partículas, una simulación CFD (Computational Fluid Dynamics) fue llevada a cabo. Para realizar una simulación CFD es importante conocer algunas propiedades de los componentes que intervienen en el proceso, para esto se realizó una simulación utilizando el Delayed Coker Model de Aspen Hysys.

Para el caso de arrastre de gotas, se realizó una simulación CFD y se encontró que es posible la formación de coque en la linea de vapor dado un caso base (conducto de salida al nivel de la superficie del reactor). Para evitar el ensuciamiento del conducto de salida se propusieron algunos cambios en la linea de vapor, los cuales consisten en introducir un fragmento del conducto al interior del reactor. Para definir la pertinencia de estas modificaciones se propusieron dos casos: introducir el conducto 30 cm y 3 m. De acuerdo con esto, se encontró que las modificaciones propuestas implican una disminución de la formación de coque. Sin embargo, no existe una diferencia muy grande entre el primer caso (30 cm) y el segundo (3 m).

Para intentar mejorar los resultados anteriores, se propuso un cambio en la geometría del reactor, la cual consiste en incrementar el diámetro del reactor en la parte superior con el fin de reducir la velocidad de las partículas lo cual puede generar un retraso en la deposición de éstas. Sin embargo, esta alternativa no mejora los resultados anteriores, sino que por el contrario incrementa la deposición de coque.

Contents

1 Introduction **1**

1.1 Motivation 1

1.2 Research problem 2

1.3 Objectives 2

1.3.1 General objective 2

1.3.2 Specific objectives 2

1.4 Thesis outline 2

1.5 State of the art 3

2 Theoretical framework **4**

2.1 Brief historical overview of the delayed coking process 4

2.2 General description of the delayed coking process 5

2.3 Thermal cracking and coke formation 6

2.3.1 Catalytic coke formation 7

2.3.2 Pyrolytic coke formation 8

2.3.3 Condensation of high boiling point components 8

2.3.4 Deposition of mechanically coke 8

2.4 Coke structure and properties 8

2.5 Kinetic mechanisms 9

3 Methodology **10**

3.1 CFD Model 10

3.1.1 Conservation equations 10

3.1.2 Turbulence modeling $\kappa - \epsilon$ 11
3.2 Operational parameters 12
3.3 Reactor 14
3.4 Physical properties 14
3.5 Simulation setup 16
3.5.1 Geometry and meshing 16
3.5.2 Boundary conditions 17
3.5.3 Kinetic mechanism 20
3.5.4 Near-wall treatment 20
3.5.4.1 Viscous sublayer 21
3.5.4.2 Buffer layer 21
3.5.4.3 Log-law region 21
3.5.4.4 Free stream flow region 21
3.5.5 Accretion model 21
3.6 Bursting Bubbles 22

4 Results **23**

4.1 Delayed Coker Model and obtaining properties of components 23
4.2 Selection of bottlenecks 26
4.2.1 Coke quality 26
4.2.2 Hot spots 27
4.2.3 Vapor line plug 27
4.3 Possible routes of plugging on the vapor line wall 28
4.3.1 Vapor line plugging by condensation 28
4.3.2 Surface velocity for coke reaction 29
4.3.3 Vapor line plugging by mechanical deposition of particles 31
4.3.3.1 CFD simulation 34

Conclusions **44**

Future Work **46**

References **47**

List of Tables

2.1 Types of thermal cracking 7

3.1 Turbulence parameters for the selected model 12

3.2 Operational conditions for coke drums reported in literature 13

3.3 Quality parameters for the mesh used in the CFD simulation 17

3.4 Physical properties of gas 19

3.5 Kinetic parameters for delayed coking reactions [1] 20

4.1 Physical properties of feed (VRC) 23

4.2 Physical properties of gas 24

4.3 Physical properties of distillates 24

4.4 Results obtained from simulation using Delayed Coker Model 25

4.5 Comparison between the main bottlenecks in the coke drum 27

4.6 Liquid fractions at 200 kPa and at different temperatures 29

4.7 Weber's number at six different droplet diameters 33

4.8 Droplet diameters at different roll-up speeds and bubble thickness 33

4.9 Summary of different cases for entered tube: tube at level with the reactor's surface, 30 cm entered tube and 3 m entered tube 39

4.10 Summary of different cases for entered tube: tube at level with the reactor's surface, 30 cm entered tube and 3 m entered tube for a new geometry 43

List of Figures

2.1 General refinery scheme 5

2.2 Process diagram for a DCU 6

2.3 Four-lump delayed coking mechanism [1] 9

3.1 Typical operational conditions for a delayed coking drum 14

3.2 Industrial drum geometry 15

3.3 Geometry of the specified zone of the drum selected for the simulation 15

3.4 Process diagram for delayed coking process using Aspen Hysys 16

3.5 Geometry and mesh used for the simulations 17

3.6 Boundaries of the geometry 18

4.1 Comparison between VRC properties according to literature (red) and VRC properties obtained using Aspen Hysys (green) 25

4.2 Comparison between product yields according to literature (red) product yields obtained using Aspen Hysys (green) 26

4.3 Possible routes for coke formation 28

4.4 Liquid fraction at different temperatures (y-axis from 400 - 420 °C) and pressures (colorbar from 180 - 225 kPa) 29

4.5 Contours of volumetric rate of coke reaction in the vapor line 30

4.6 Contours for values of y_2 31

4.7 Surface reaction rate 31

4.8 Distillation curves for VRC 32

4.9 Droplets behavior according to the Weber's number and wall temperature . 33

4.10 Mesh independence in cylinder section 34

4.11 Mesh independence in vapor line section 35

4.12 Trajectory base case: tube at level with the reactor's surface 35

4.13 Deposition rate of particles for Base case: tube at level with the reactor's surface 36

4.14 Trajectory of the particles for a 30 *cm* entered tube 36

4.15 Deposition rate of particles for 30 *cm* entered tube 37

4.16 Trajectory of the particles for a 3 *m* entered tube 37

4.17 Deposition rate of particles for a 3 *m* entered tube 38

4.18 Coke drum with variable diameter 40

4.19 Trajectory of the particles for tube at level with the reactor's surface in a coke drum with variable diameter 40

4.20 Accretion rate of particles for Base case: tube at level with the reactor's surface 41

4.21 Trajectory of the particles for a 30 *cm* entered tube in a coke drum with variable diameter 41

4.22 Accretion rate of particles for 30 cm entered tube in a coke drum with variable diameter 41

4.23 Trajectory of the particles for a 3 *m* entered tube in a coke drum with variable diameter 42

4.24 Accretion rate of particles for 3 m entered tube in a coke drum with variable diameter 42

Chapter 1
Introduction

This chapter introduces to the reader to the delayed coking process and the motivation of this research showing the importance of this process in the Colombian refineries. In this chapter the research problem is proposed, as well as the objectives of this thesis.

1.1. Motivation

Traditionally in the petrochemical industry only light crude oils had been extracted and refined because of the low prices of these processes. However, recently the extraction of heavy crude oils has increased due to the growing demand of petroleum fuels and the decrease of light hydrocarbons reserves. Particularly, according to a report made for the Colombian Mining and Energy Planning Unit (Unidad de Planeación Minero Energética: UPME), Colombia tends to increase the production capacity of heavy oil in the next 20 years taking into account three scenarios: a base case, a shortage case and an abundance case [2]. In Colombia the refineries were originally built for the upgrading of mid and light crude. However, recently over half of the crude produced is heavy and extra-heavy crude oil. With this in mind, an update process technologies is needed [3]. For this reason Ecopetrol developed a modernization of the refining process which, is called El Plan Maestro de Ecopetrol [4]. One of the scopes of El Plan Maestro de Ecopetrol is an expansion and modernization of Reficar refinery, this expansion includes the start-up of a delayed coking unit (DCU) for the treatment of the bottom of the barrel fractions. In February 2016 began operations of Reficar refinery which has a capacity of 165000 bpd, it is the most modern refinery of Latin America. The delayed coking unit has a capacity of 43000 bpd and due to its implementation coke is produced in Colombia for the first time. The DCU produces 2500 ton/day of coke which is exported.

Some of the advantages in the operation of a delayed coking unit are that delayed coking has a high-efficiency thermal deasphalting of petroleum residues, reducing the contents of metals in the samples and it is not limited by the quality of the feed [5]. The fact that a DCU has not limitation for the treatment of any type of petroleum residue implies a better use of the resources and enhance of the overall efficiency of the refinery.

In the delayed coking process, the most important part is the coke drum in which the residue is converted into light products. For an appropriate operation of the process, it is important to identify and to correct bottlenecks in the coke drum since an unsuitable operation can lead to failures in the reactor, or even accidents.

1.2. Research problem

There are different options for refining heavy oil fractions such as Eureka process, visbreaking, fluid coking, flexi-coking or delayed coking [3; 5; 6]. Delayed coking has some advantages such as a high conversion and the fact that any type of crude can be treated. The role of a delayed coking unit (DCU) is to convert any residue, usually vacuum residue crude (VRC), into more valuable products: fuel gas, LPG, naphtha and gasoil [7; 8; 9; 10].

The first DCU was built in 1929 by Standard Oil of Indiana [8], but since then the delayed coking has not been widely studied because of the availability of light crude and the high costs of treating heavy crude oils. Therefore, as a conclusion of the above-mentioned and the review of the state of the art, it is possible to say that the academic literature related with delayed coking is descriptive.

The industrial delayed coking process is very complex and during the operation of a DCU some bottlenecks could appear, such as formation of hot spots, streams plugging, foam formation, etc. Therefore the laboratory approximations have limited application for an industrial scale [11]. As far as the author know, a CFD simulation has not carried out up to date. The CFD simulation approach is proposed to avoid bottlenecks and to obtaining appropriated operational parameters for a coke drum.

1.3. Objectives

1.3.1. General objective

To propose design alternatives to improve the operation of a delayed coking drum using computational fluid dynamics.

1.3.2. Specific objectives

1. To develop a CFD simulation for understanding the operation of a coke drum in a delayed coking unit.
2. To identify the main bottlenecks for a coke drum in a delayed coking unit.
3. To evaluate design alternatives to improve the operation of an online coke drum in a delayed coking unit.

1.4. Thesis outline

The main purpose of this thesis is to present an improvement of the performance of a coke drum. To reach this purpose, a literature review was made to select the main bottlenecks of the process. Once the bottleneck is selected, a CFD simulation was carried out to analyse the possible causes of the selected bottleneck. With this in mind, a design alternative

is proposed with the aim of reduce the effect of the selected bottleneck. Considering the reduced information about the delayed coking process, a first approximation of the improvement of the unit is proposed.

1.5. State of the art

This thesis presents a possible improvement for the operation of the coke drum of a delayed coking unit. For the study of the possible inefficiencies of the process and for possible solutions a CFD simulation was carried out. For the development of this thesis, a literature review was made.

According to the literature review, the information about delayed coking process is reduced. In Colombia Díaz-Mateus [3] develop a CFD simulation of a pilot reactor to predict the product yields. Additionally, in Colombia Meléndez et al. [12] characterized some samples of vacuum residue by infrared spectroscopy with attenuated total reflectance (FTIR-ATR) and principal component analysis (PCA).

Taking into account the literature review, there are not many studies about the bottlenecks of this process. Considering that the selected bottleneck is the vapor line plugging because of coke deposition, some information for a similar case was considered. S. De Schepper et al [13] develop a model for the coke formation in convection section tubes of steam crackers and assume that the deposition is because of impinging drops of heavy hydrocarbons.

Chapter 2
Theoretical framework

The components which are part of the delayed coking process are a main fractionator, a couple of parallel adiabatic coke drums which operate in a semi-continuous process and a furnace [8; 10; 14]. In delayed coking process the VRC is heated in a furnace until the coking temperature is reached ($< 500°C$) and the VRC is taken to the online coke drum in which the coking reactions are carried out and light hydrocarbons and coke are produced [8] . Light hydrocarbons are treated later in other units for the production of valuable products such as gasoline and diesel, and coke can be used as fuel or in steel production [3; 8; 14].

2.1. Brief historical overview of the delayed coking process

The first petroleum coke was produced in 1860 in order to obtain kerosene which was used for lighting. For this purpose iron stills were used for boiling the crude oil until coke formation. After the distillation has been made, the still was cooled and an operator dug out the coke before the next run. In 1880 stills in series were used to obtain a stage separation of different components and the petroleum coke was produced only in the first still [8].

Later, in 1920, a process with a tube furnace and a separation column was built. The bottoms from the column were taken to a wrought iron still in which the whole outside still was in direct contact with the flue gases. This arrangement was used to obtain a high quantity of heavy gasoil. For the coke extraction the operators used picks and shovels and they had to cover their head to protect themselves against the heat from the still [8].

The first DCU was built in 1929 by Standard Oil of Indiana but there was not a mechanical tool for decoking drums. Subsequently, in 1930's a hydraulic decoking system was developed by Shell Oil at Wood River, Illinois [8].

Before 1955 the number DCUs were small. However the building of DCUs between 1955 and 1970 increased by 6% per year [8]. The number of DCUs tends to grow with the increasing number of FCC units and the reduction in the number of processes that apply thermal cracking [8]. During the period between 1999 and 2005 the global coking capacity increased by 23%, equivalent to 47.3 millions of tons [5].

2.2. General description of the delayed coking process

For the analysis of delayed coking it is important to understand how a refinery works. The refinery's feedstock is the crude oil which contains around 0.2% of water and dissolved salts. For this reason, the crude oil should be desalted. The desalted crude is heated up in a furnace above 658 K and it is taken to an atmospheric column in which products such as naphtha, kerosene, diesel, jet fuel, Light Atmospheric Gasoil (LAGO) and Atmospheric Reduced Crude (ARC) are obtained. The ARC is heated to around 368 K and taken to a vacuum distillation tower. The outlets of this tower are Heavy Vacuum Gasoil (HVGO) and Vacuum Reduced Crude (VRC). The delayed coking process upgrades the VRC into light ends, naphtha, Light Coker Gasoil (LCGO) and Heavy Coker Gasoil (HCGO), and produces coke as a byproduct. HCGO, HVGO and LAGO are taken to a Fluid Catalytic Cracking Unit (FCCU) wherein products such as gasoline, diesel and light ends are obtained [9; 10; 14; 15; 16]. In Fig. 2.1 a general refinery scheme is shown.

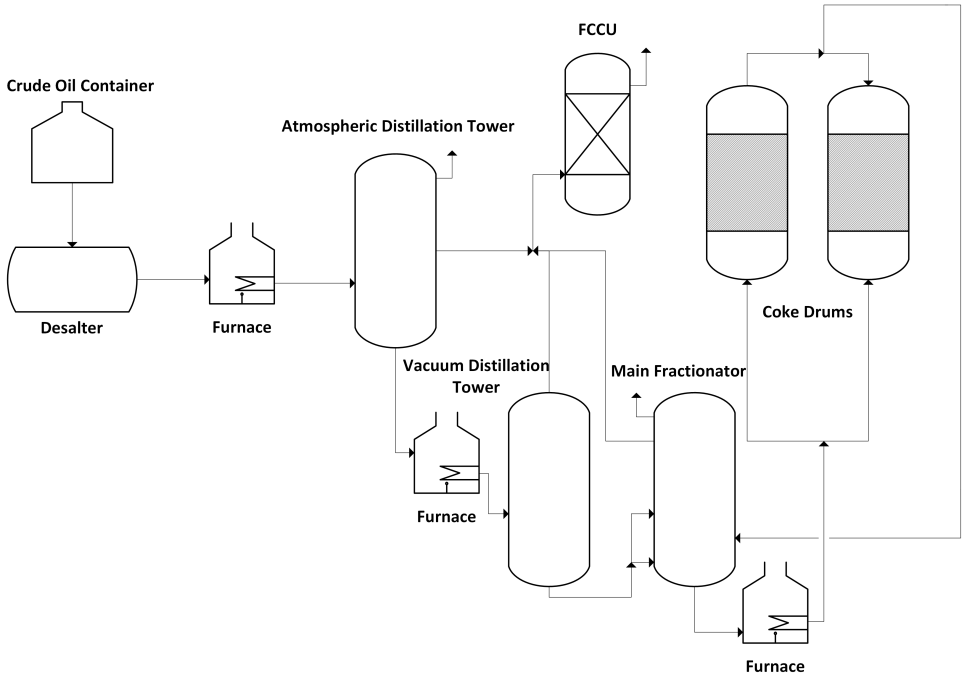

FIGURE 2.1. General refinery scheme

Each parallel adiabatic coke drum has a diameter around 4-9 meters (13-30 ft.) and a height of the order of 25 meters (82 ft.). Usually the drum walls are 25 mm carbon steel with an internal layer of 2.8 mm stainless steel as a protector against sulfur corrosion [8]. The scheme of a DCU in fig. 2.2 was the result of summarizing the typical features of cokers described in the literature [8; 9; 14; 17; 18].

The coke drum is the main equipment in a DCU because it converts a residue into more valuable products which are later separated in the main fractionator [7; 8; 9; 10; 14]. The main fractionator has two inlet streams: stream 1 with VRC and stream 5 with high-temperature reaction gas from the coke drum [10]. The bottoms of the main fractionator (stream 2) are taken to the furnace where are heated up and then the outlet stream is carried out to one of the coke drums. To avoid coking within the furnace, high pressure

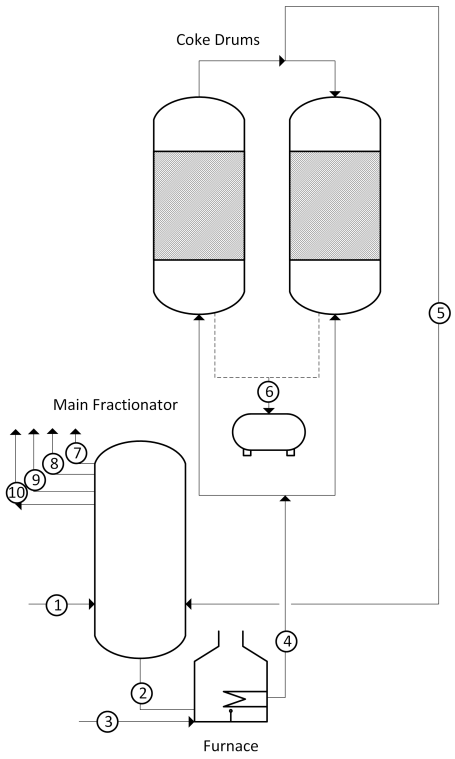

FIGURE 2.2. Process diagram for a DCU

steam could be injected before the furnace (stream 3) [7]. Then the stream 4 coming from the furnace goes into the coke drum. The stream 5 is the coke drum outlet. That stream transports the products to the main fractionator where it is separated in light ends, Coker Naphtha (CN), Light Coker Gasoil (LCGO) and Heavy Coker Gasoil (HCGO) (Streams 7, 8, 9 and 10 respectively). The residence time of the vapors inside the coke drum varies between 60-300 seconds [19].Once the online coke drum is full of coke the feed is switched to an empty parallel drum while the coke is extracted (stream 6).

The cycle of a coke drum varies 12-24 hours. During this time the offline drum undergoes different processes: steam stripping, water cooling and water draining, opening, hydraulic decoking, closing and testing and preheating.

2.3. Thermal cracking and coke formation

Thermal cracking is a thermal process which transforms heavy residue into light components using high temperatures. This process could forms coke as byproduct. The lighter products are the result of the cracking reactions which are part of the initialization reactions and this products have a low quantity of sulfur because most of it is retained in coke. On the other hand, the coke formation is part of the final step of the route [20].

Routes related to the growth and coke formation are similar for coils, heat exchangers and delayed coking drums. The coke formation on the surfaces of those refinery equipment

could cause inefficiencies in the process. The coke formation on surfaces could be carried out at temperatures over 300 $°C$. [21].

There are three types of thermal cracking with coke formation: mild thermal cracking, moderate thermal cracking and severe thermal cracking.

When mild cracking is used, the heating process for the cracking is mild. This process is used to obtain viscosity reduction and to produce lighter products. The operational temperature is between $471 - 493$ $°C$, the pressure is between $300 - 1300$ kPa and the coke yield is around 10%. The characteristic process of mild thermal cracking is visbreaking process [20].

In the case of moderate thermal cracking, the characteristic process is delayed coking process. The coke yield is around 30%, the operational temperature is around $450 - 515$ $°C$ and the pressure is between $35 - 700$ kPa [20; 22; 23].

The characteristic processes of severe thermal cracking are fluid coking and flexicoking processes. In this case the residue is cracked at high temperatures ($482 - 566$ $°C$). In the case of fluid coking, part of the coke formed is burned and it is used to heat the feed to the reactor. For the flexicoking process, vapor is used for the gasification of most of the coke. The operational pressure is around 700 kPa and the coke yields are 20% and 2% for fluid coking and flexicoking respectively [20].

TABLE 2.1. Types of thermal cracking

Type of thermal cracking	**Characteristic process**	**Temperature range ($°C$)**	**Pressure range (kPa)**	**Coke yield (%)**
Mild thermal cracking	Visbreaking	$471 - 493$	$300 - 1300$	10
Moderate thermal cracking	Delayed Coking	$450 - 515$	$35 - 700$	30
Severe thermal cracking	Fluid coking and Flexicoking	$482 - 566$	700	20 for fluid coking and 2 for flexicoking

There are four main routes of coke formation: catalytic coke formation, pyrolytic coke formation, condensation of high boiling point components and mechanical deposition of coke [24; 25]. The four routes are described below.

2.3.1. Catalytic coke formation

It is refered to the coke formation due to catalytic effect of the metallic surface [21; 24; 25; 26; 27; 28; 29; 30; 31]. Often the catalytic surface is the refinery equipment wall. The coke formation on catalytic surfaces could appear at low temperatures (around 500 $°C$) [24; 25]. The catalytic coke formation generates a thin layer of coke, around 50 - 60 μm. In this zone appear fiber structures with diameters of some microns and lengths of tens of microns. Because of the fiber structure, this zone void fraction predominates and

the thermal conductivity is reduced. The fibers formation is generated mainly because of vinyl components. The addition of the vinyl components in the catalytic surface form polymeric fibers with a metallic head. The metallic head is extracted from the wall and it is a new active site but in the fiber[21]. The metallic extraction cause deformations on the surface increasing the surface area, hence increasing the active sites on the metallic wall of the equipment [24; 25].

2.3.2. Pyrolytic coke formation

It is related to the coke formation in the gas phase. The coke is formed rapidly in the gas phase and then it generates a deposit on the walls. It predominates at high temperatures processes with light feed, such as ethane cracking. In this case the coke formation is because of radicals presence which are coke precursors [24; 25; 26; 31].

2.3.3. Condensation of high boiling point components

Condensation predominates at low temperatures and relatively heavy components from another process outlet. Because of the low temperatures a kind of fog is formed which is added to the equipment surfaces generating a carbonaceous deposit because of dehydrogenation reactions of it. Part of the non-condensed fog suffers dehydrogenation reactions in the gas phase forming particles in gas phase which can be deposited later [24; 25; 31].

2.3.4. Deposition of mechanically coke

There are three types of particles which could be shifted coke fibers detached from a metallic surface, pyrolytic coke formed in a gas phase stream and remaining coke particles from cleaning stages [24; 25].

2.4. Coke structure and properties

The coke is formed from the bottom of the drum to a top line specified by the user. At first the coke is formed around a main channel whereby flows the liquid phase. As the coking progress the main channel is converted into randomly branches and later these channels are divided into more branches with smaller diameters [32].

The delayed coke could have three physical structures which depend on the VRC properties and operational conditions of the reactor. The physical coke structures are as follows: shot, sponge and needle [3; 8; 14; 22]. The use of the coke depends on its properties and structure. Fuel grade coke is used as fuel, aluminum grade coke is calcined for the use in the aluminum industry and the graphite grade coke is used in the production of graphite electrodes used in electric arc furnaces by the steel industry [3; 8; 14].

2.5. Kinetic mechanisms

The number of kinetic mechanisms that describe the delayed coking reactions available in the literature is limited. Therefore, modelers of DCU tend to adjust mechanisms developed for similar processes that form coke such as visbreaking and thermal cracking.

In the refereed literature only one mechanism describes the delayed coking process [33]. This mechanism involves 11 lumps and a SARA methodology is employed. This mechanism predicts the yield of naphtha at the end of the reactor.

In literature there are mechanisms for residua decomposition [22; 34; 35; 36]. To simplify the representation of the components and reactions, the authors groups the components in lumps and pseudo-components.

The mechanisms proposed by Del Bianco et al. and Sawarkar et al. are four-lumps kinetic mechanisms which involves first order reactions, and vacuum residue, distillates and coke as common lumps. For the mechanism proposed by Del Bianco et al. the fourth lump is an intermediate between residue and coke and the Sawarkar et al. mechanism does not take into account any intermediate and they consider gas as a fourth lump [22; 34].

On the other hand, Köseoglu & Phillips proposed a six-lump mechanism in which a SARA methodology was employed for the product characterization. Later Mendonça Filho proposed a modification for that mechanism which involves an intermediate [35; 36].

López-Pérez propose a three reactions and four lump mechanism which includes VRC, distillates, gas and coke (Fig. 2.3). For this purpose López-Pérez assume the coker drum as a batch reactor [1]. It is the closest mechanism and was selected for the case of study.

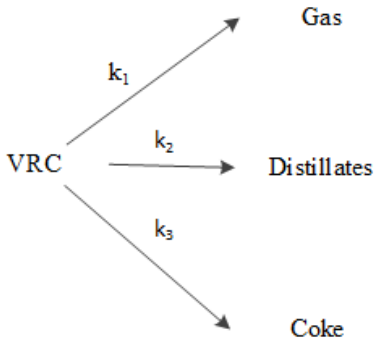

FIGURE 2.3. Four-lump delayed coking mechanism [1]

Chapter 3
Methodology

According to the objectives of this thesis, a methodology is proposed to reach these. This chapter presents the mathematical model related to the CFD model such as conservation equations and turbulence model. It is important to know the input for the simulation, thus, the operational parameters, boundary conditions, kinetic mechanism and geometry and are presented. Other issues to take into account are how the coke formation is and how to model it. For this purpose a model related to near wall behavior of the fluid.

3.1. CFD Model

3.1.1. Conservation equations

Mass conservation equation

According to the mass conservation law, the continuity equation is obtained as is shown in Eq. 3.1. It is possible to use this equation for compressible and incompressible flow:

$$\frac{\delta \rho}{\delta t} + \nabla \cdot (\rho \overrightarrow{v}) = 0 \tag{3.1}$$

Where ρ is the fluid density.

Taking into account that the coke drum operates in stady state, the Eq. 3.1 is simplified as follows in Eq. 3.2

$$\nabla \cdot (\rho \overrightarrow{v}) = 0 \tag{3.2}$$

Momentum conservation equation

The momentum conservation equation is shown below (Eq. 3.3)

$$\frac{\delta}{\delta t}(\rho \overrightarrow{v}) + \rho \nabla \cdot (\overrightarrow{v}\,\overrightarrow{v}) = -\nabla p + \nabla \cdot \tau \tag{3.3}$$

Where v is the flow velocity, p is the pressure, τ is the stress tensor, ρ is the density of the fluid and ρg is the gravitational force.

Taking into account that the coke drum operates in steady state, the Eq. 3.3 is simplified as follows in Eq. 3.4

$$\nabla \cdot (\overrightarrow{v}\,\overrightarrow{v}) = \frac{1}{\rho}(-\nabla \cdot p + \nabla \cdot \tau) \tag{3.4}$$

τ is defined as (Eq. 3.5):

$$\tau = \mu\big[(\nabla \cdot \overrightarrow{v} + \nabla \cdot \overrightarrow{v}^{T}) - \frac{2}{3}\nabla \cdot \overrightarrow{v} I\big] \tag{3.5}$$

Where μ is the molecular viscosity and I is the unit vector.

Energy conservation equation

From the energy conservation law at steady state, is obtained the transport energy equation as is shown in Eq. 3.6:

$$\nabla \cdot (\overrightarrow{v}T) = \frac{-k}{\rho C_p}\nabla^2 \cdot T \tag{3.6}$$

3.1.2. Turbulence modeling $\kappa - \epsilon$

Turbulence Kinetic Energy (TKE)equation

The equation of Turbulence Kinetic Energy (TKE) is given by Eq. 3.7:

$$\frac{\delta(\rho\kappa)}{\delta t} + \frac{\delta(\rho\kappa\overline{v_i})}{\delta x_i} = \frac{\delta}{\delta x_i}\left(\frac{\mu_t}{\sigma_k}\frac{\delta\kappa}{\delta x_i}\right) + \rho\overline{v_i'v_j'}\frac{\delta\overline{v_j'}}{\delta x_i} - \rho\epsilon \tag{3.7}$$

Rate of Dissipation

It is given by Eq. 3.8:

$$\frac{\delta(\rho\epsilon)}{\delta t} + \frac{\delta(\rho\epsilon\overline{v_i})}{\delta x_i} = \frac{\delta}{\delta x_i}\left(\frac{\mu_t}{\sigma_\epsilon}\frac{\delta\epsilon}{\delta x_i}\right) + \frac{\epsilon}{\kappa}(c_{\epsilon 1}P^{\kappa} - c_{\epsilon 2}\epsilon) \tag{3.8}$$

For Eq. 3.7 and 3.8, the first term at the left side represents the rate of change of κ and ϵ respectively. The second one is the convective term for each case (κ and ϵ). At the

right side there are three terms: the diffusion term, rate of production term and rate of destruction for κ and ϵ respectively.

The terms σ_k, σ_k, $c_{\epsilon 1}$ and $c_{\epsilon 1}$ are turbulence parameters for the model. The typical values for these parameters are shown in Table 3.1.

TABLE 3.1. Turbulence parameters for the selected model

$\sigma_\kappa = 1.0$	$\sigma_\epsilon = 1.3$	$c_{\epsilon 1} = 1.4$	$c_{\epsilon 2} = 1.9$

3.2. Operational parameters

Usually, the aim of a DCU in a refinery is to produce the maximum possible liquid yields with low coke production. The liquid yields depend on operational parameters of the unit such as temperature, pressure and recycle. Typically for each 100 tons of HCGO converted, 20-50 tons coke may be produced, depending on the operational conditions employed for the coke drum [37].

For the determination of typical operational conditions for the coke drum, a literature review was carried out, which includes tutorials, patents and academic and gray literature. Table 3.2 summarizes the operational conditions reported in literature, where the red lines represent the data from literature and the green ones represents the mean value. Fig. 3.1.a shows the standard values for the inlet temperature ($450 - 515°C$) and the mean value for this condition is $482.5°C$. Fig. 3.1.b shows the typical values for the outlet reactor temperature, which is between $415 - 482°C$, and the mean value is $448°C$. Fig. 3.1.c shows the typical values for the operational pressure. Pressure has a wide operational range between $35 - 700$ kPa and the mean value is 230 kPa. Finally, Fig. 3.1.d represents the typical data for the recycle ratio. The recycle ratio is between $0\% - 70\%$ and these values depends on the feed quality: a high quality feed requires less recycle and a low quality feed requires a high recycle. For high quality feed the mean value is 17%.

TABLE 3.2. Operational conditions for coke drums reported in literature

Reference	**Inlet temperature (°C)**	**Outlet temperature (°C)**	**Pressure (kPa)**	**Recycle**	**Feed flow (t/h)**
Ellis et al., 1998	500	443	$200 - 300$	NR	NR
Chen et al., 2004	< 500	NR	NR	NR	62.5
Sawarkar et al., 2007	$480 - 515$	$415 - 465$	$100 - 400$	NR	NR
McKetta et al., 1992	$488 - 502$	$432 - 449$	$172 - 275$	10%	NR
Tian et al., 2012	$480 - 500$	NR	$150 - 180$	$0\%; 15\%; 30\%$	9×10^{-4}
Holden et al., 2014	490.5	452.8	200	NR	220
Bloomer et al., 1971	$482 - 515$	$449 - 482$	NR	$30\% - 60\%$	30.7
Dabkowski et al., 1987	$450 - 500$	NR	$35 - 700$	$10\% - 30\%$ (High quality feed) $30\% - 70\%$ (Heavier feed)	NR
Kapustin et al., 1983	$450 - 470$	NR	100	$20\% - 60\%$	NR

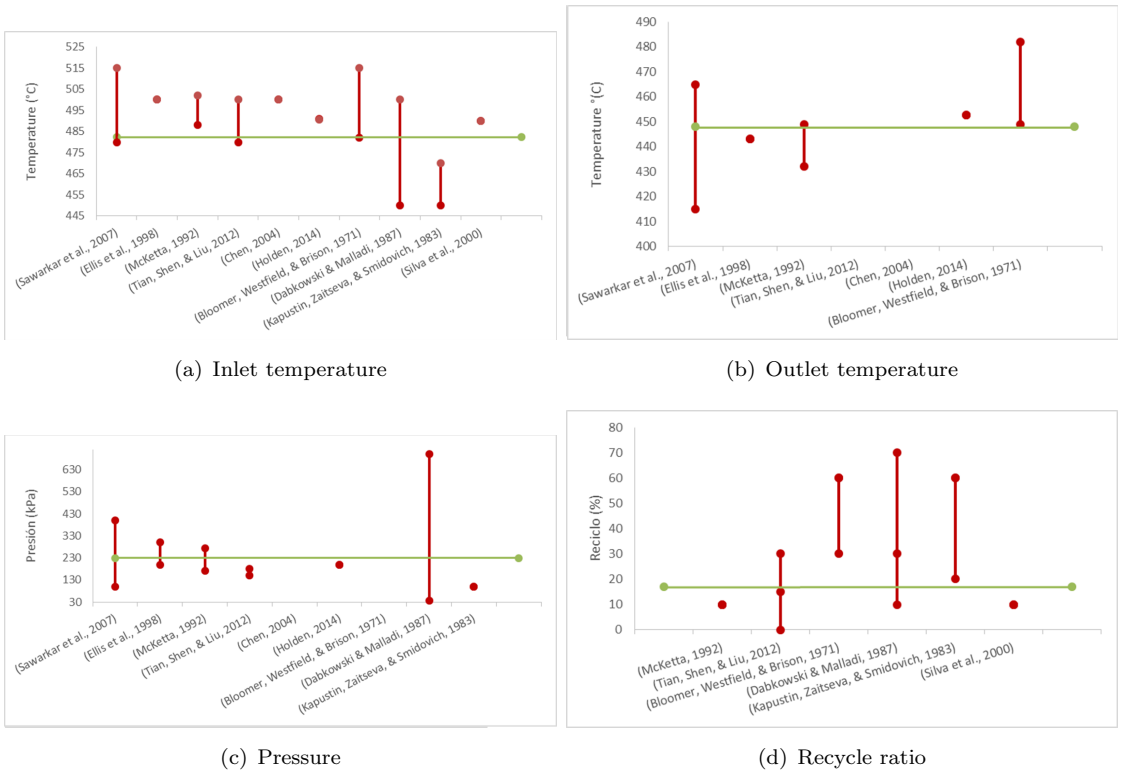

(a) Inlet temperature

(b) Outlet temperature

(c) Pressure

(d) Recycle ratio

FIGURE 3.1. Typical operational conditions for a delayed coking drum

3.3. Reactor

The coke drum has a cylindrical shape with two flanges at the top and at the bottom for the cleaning process. The diameters of the superior and inferior flanges vary between 1.5 and $2m$ respectively [8]. The top of the drum has a rounded shape and the bottom has a conic shape and under the cone there is a cylindrical support [39]. Oka et al, report the dimensions of an industrial scale drum; however they do not report the diameter of the superior flange. Fig. 3.2 presents the geometry for a coke drum based on the data from [8; 39].

The established temperature and pressure conditions are $447°C$ and $200kPa$ respectively. As will be explained Section 4.2, the approach of the simulation will be the top of the reactor, including the vapor line. Fig. 3.3 shows the geometry of the specified zone of the drum selected for the simulation.

3.4. Physical properties

According to the kinetic mechanism selected for the simulation of the drum, the components in the vapor phase are VRC, distillates and gas. Because of the temperature difference in the reactor is not significant, the physical properties of the components are assumed as constant. The physical properties of the components were obtained from the

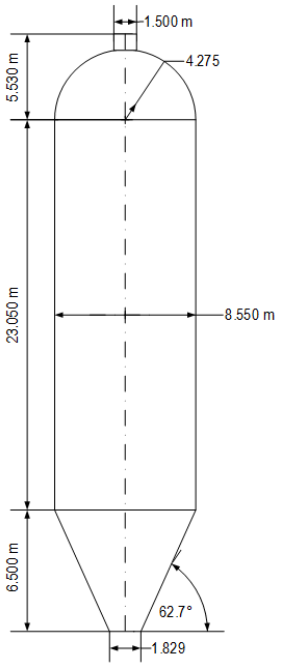

FIGURE 3.2. Industrial drum geometry

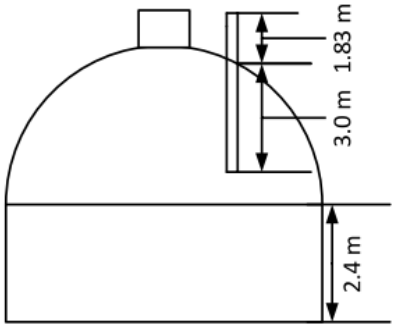

FIGURE 3.3. Geometry of the specified zone of the drum selected for the simulation

Delayed Coker Model from Aspen Hysys. The physical properties of the components of the process used for the CFD.

To obtain the properties of coke drum products, a simulation using the Delayed Coker Model from Aspen Hysys was carried out. To develop the simulation it is necessary to characterize the feed using the option *Petroleum Assays* and using as inlet the data such as TBP, sulfur content, density, and nitrogen and vanadium contents taken from [40]. The results of the feed characterization was showed in the last chapter.

Once the feed characterization was made, the Delayed Coker Model was calibrated. For the calibration of the model data from [40; 41] was employed. The diagram of the simulation is shown in Fig. 3.4. The operational conditions established for the model was taken as the average value from the data showed in Fig. 3.1.

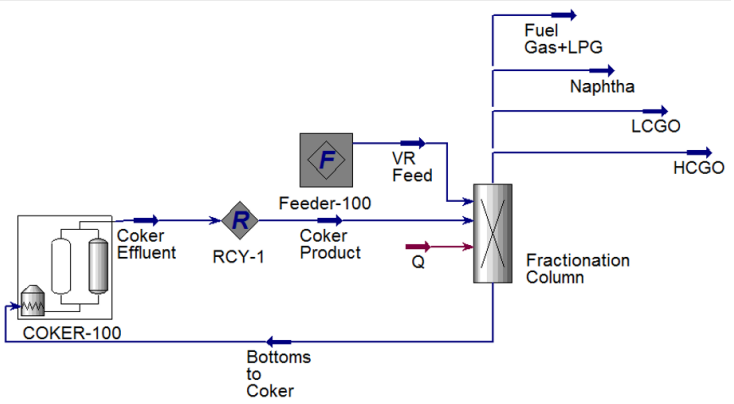

FIGURE 3.4. Process diagram for delayed coking process using Aspen Hysys

3.5. Simulation setup

3.5.1. Geometry and meshing

ANSYS ICEM CFD pre-processing software was used to develop the discretization of the 3D geometry. Later, a mesh was created using tetrahedral elements, approximately 950000. Fig. 3.5 shows the geometry and mesh used for simulations. Other meshes were created to evaluate mesh independence as is shown in the next chapter. Five meshes were evaluated with around of 247000, 485000, 755000, 950000 and 1400000 elements respectively.

To evaluate the mesh quality, the aspect ratio and equiangle skewness were evaluated. According to the ANSYS ICEM CFD help manual, to obtain a good mesh quality those parameters should tend to 1. Table 3.3 shows the values for aspect ratio and equiangle sqewness obtained for the used mesh.

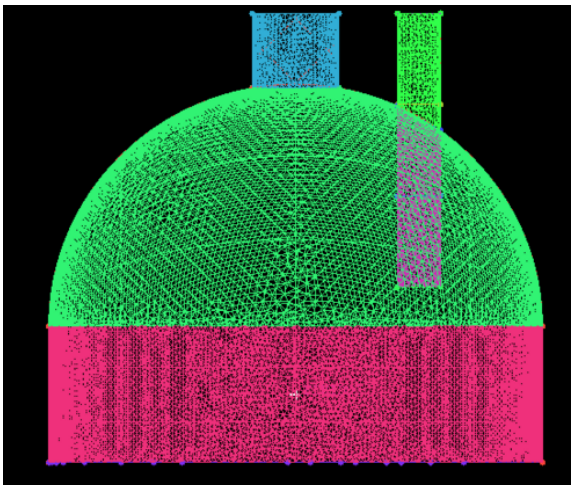

FIGURE 3.5. Geometry and mesh used for the simulations

TABLE 3.3. Quality parameters for the mesh used in the CFD simulation

Quality parameter	Range of values	Recommendation
Aspect ratio	0.4 - 1 (80% of the elements between 0.9 - 0.95)	$\rightarrow 1$
Equiangle sqewness	0.3 - 1 (77% of the elements between 0.9 - 0.95)	$\rightarrow 1$

3.5.2. Boundary conditions

To define the type of boundary conditions is important to delimit each zone of the geometry (Fig. 3.6). According to Fig. 3.6, there are three boundaries defined as "Wall", there is one boundary defined as "Velocity Inlet" and one defined as "Outflow". The boundary conditions for each zone are shown in Table 3.4

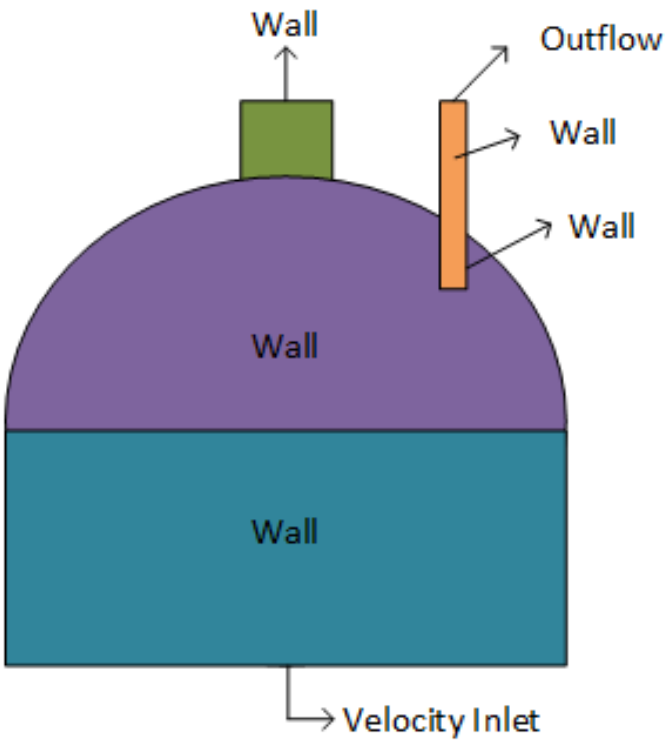

FIGURE 3.6. Boundaries of the geometry

TABLE 3.4. Physical properties of gas

Type of Condition: Wall				
Zone	**Momentum**	**Thermal**	**Species**	**DPM**
cilindro	Stationary Wall No Slip Roughness Height(m): 0 Roughness Constant: 0.5	Convection Heat Transfer Coefficient ($Wm^2 - K$): 25 Free Stream Temperature (K): 300 Heat Generation Rate (W/m^2): 0	Zero Diffusive Flux (C) Zero Diffusive Flux (VRC) Diffusive Flux (Gas)	Reflect
cilindroDrill	Stationary Wall No Slip Roughness Height(m): 0 Roughness Constant: 0.5	Convection Heat Transfer Coefficient ($Wm^2 - K$): 25 Free Stream Temperature (K): 300 Heat Generation Rate (W/m^2): 0	Zero Diffusive Flux (C) Zero Diffusive Flux (VRC) Diffusive Flux (Gas)	Reflect
semiesfera	Stationary Wall No Slip Roughness Height(m): 0 Roughness Constant: 0.5	Convection Heat Transfer Coefficient ($Wm^2 - K$): 25 Free Stream Temperature (K): 300 Heat Generation Rate (W/m^2): 0	Zero Diffusive Flux (C) Zero Diffusive Flux (VRC) Diffusive Flux (Gas)	Reflect
pared_salida	Stationary Wall No Slip Roughness Height(m): 0 Roughness Constant: 0.5	Coupled	Zero Diffusive Flux (C) Zero Diffusive Flux (VRC) Diffusive Flux (Gas)	Trap
pared_salida_int	Stationary Wall No Slip Roughness Height(m): 0 Roughness Constant: 0.5	Coupled	Zero Diffusive Flux (C) Zero Diffusive Flux (VRC) Diffusive Flux (Gas)	Trap
Type of Condition: Velocity Inlet				
inlet	Magnitude, Normal to Boundary Velocity Magnitude (m/s): 0.2191 Turbulence Intensity (%): 0.025 Hydraulic Diameter (m): 8.25	Temperature (K): 720	Mass Fraction(C): 0 Mass Fraction (VRC): 0.0119 Mass Fraction (Gas): 0.0588	

3.5.3. Kinetic mechanism

According to Section 2.5, the mechanism proposed in [1] is the closest mechanism for delayed coking process. The kinetic parameters are shown in Table 3.5.

TABLE 3.5. Kinetic parameters for delayed coking reactions [1]

Reaction	**Ea** (kJ/mol)	**Ln Ko** $(1/h)$
1	219.71	34.90
2	171.73	27.78
3	268.02	44.06

The mechanism proposed is considered for a volumetric reaction, however in vapor line, surface reactions are the more important according to Section 2.3. For this reason it is necessary to convert volumetric coke formation reaction into a surface reaction. Therefore it is important to take into account the behavior of the fluid near to the wall such as is shown in Section 3.5.4. The derivation of surface reaction velocity is developed in Section 4.3.2

3.5.4. Near-wall treatment

When the effects near to wall are relevant it is important to take into account a near wall treatment to obtain a better approximation in this zone. There are four flow regions: viscous sublayer, buffer layer, log-law region and free stream flow region. The regions can be represented using a dimensionless length $Y+$.

$Y+$ is an dimensionless quantity which relates the effects of the viscosity in the near-wall flow. It is analogue to the Reynolds number, but $Y+$ takes into account the velocity near to the wall and the near wall distance. $Y+$ is defined as is shown in equation 3.9 [42].

$$Y+ = \frac{\rho u_\tau y}{\mu} \tag{3.9}$$

Where ρ is the fluid density, y is the near wall distance, μ is the dynamic viscosity and u_τ is the so-called friction velocity it is the near wall velocity related to the viscous effects and is defined as is shown in equation 3.10.

$$u_\tau = \sqrt{\frac{\tau_w}{\rho}} \tag{3.10}$$

Where τ_w is the wall shear stress. The SI unit for this quantity is Pa and it is defined as:

$$\tau_w = \mu \frac{\partial u}{\partial y} \tag{3.11}$$

3.5.4.1. Viscous sublayer

It is also called laminar sublayer. It is known that the velocity in the wall is zero, however exists a small region above of it in which the flow is laminar, this zone is the viscous sublayer. The characteristic $Y+$ values for this zone are $Y+ < 5$ [42; 43].

3.5.4.2. Buffer layer

It refers to the zone where exist a transition between laminar flow and turbulent flow. The length of this layer from the wall is δ, it means the boundary layer. The characteristic $Y+$ values for this zone are $5 < Y+ < 30$ [43].

3.5.4.3. Log-law region

In this zone the flow is totally turbulent. In this region the mean velocity is proportional to the logarithm of the distance in the same zone ($u+ = \frac{1}{k}\ln(Y+)+b$). The characteristic $Y+$ values for this zone are $30 < Y+ < 500$ [42].

3.5.4.4. Free stream flow region

The viscous effects in this zone are neglected. The characteristic $Y+$ values for this zone are $Y+ < 500$ [42].

3.5.5. Accretion model

To study the droplets (particles) behavior and its deposition, particles from the inlet are injected and the trajectories were evaluated. For this purpose a Discrete Phase Model (DPM) was selected. DPM can be setted according several physical models.

For mechanical deposition of droplets the accretion model of DPM was selected. The accretion rate is defined as:

$$R_{accretion} = \sum_{p=1}^{N_{particles}} \frac{\dot{m}}{A_{face}} \tag{3.12}$$

Where $\dot{m}$ is the mass flow of the each particle and A_{face} is the cell face area. Eq. 3.12 represents the mass rate of droplets deposition per area.

The boundary condition for the inner wall of the vapor line is “trap”, and “reflect” for the other walls.

3.6. Bursting Bubbles

For the coke formation by mechanical deposition, it was considered that the impinging drops are produced because of bursting bubbles. There is not available literature about bursting bubbles on crude, then to evaluate the droplet diameters from bursting bubbles an approximation from [44] was made. D. Spiel [44] describes a model for births drops from bursting bubbles on seawater surfaces. According to this model, the diameter of the drops (D_d) from bursting bubbles depends on the thickness of bubble, surface tension and density. Eq. 3.13 shows the adjusted model for VRC, considering its properties.

$$D_d = 2 * 3.57 \left\{ \frac{2 * 4.1312 \times 10^8 \rho (1 - \cos(31.3))}{S_f^2 \rho \pi \sin(31.3)} \right\}^{1/2} \tag{3.13}$$

Where S_f is the film roll-up speeds (m/s). S_f is defined as (Eq. 3.14):

$$S_f = \left(\frac{2\gamma}{h\rho} \right)^{1/2} \tag{3.14}$$

Where h is the film thickness which range is between 0.3 and 3 μm.

Chapter 4
Results

This section presents the results of this research such as the analysis of bottleneck and the selection of the more representative one. The selected bottleneck is the plugging of vapor line because of the coke formation. Taken into account the selected bottleneck, the possible causes were analyzed and evaluated. The possible causes analyzed were vapor line plugging by condensation, by chemical reaction and by deposition.

4.1. Delayed Coker Model and obtaining properties of components

To develop a CFD simulation it is necessary to obtain some properties of components of delayed coking process. However, most of these properties for the delayed coking components are not available in literature, hence a simulation using the Delayed Coker Model of Aspen Hysys was carried out to obtain these properties, according to Section 3.5.2. The physical properties of feed (VRC), gas and distillates are shown in Table 4.1. According to a literature review, the values of mass density, conradson carbon and molecular weight were validated for VRC and for gas and distillates, the values for molecular weigh were validated. However, there are not more information about other properties which are necessary for CFD simulations, such as mass heat capacity, mass heat of vaporization, surface tension, thermal conductivity and viscosity.

Table 4.1. Physical properties of feed (VRC)

VRC	
Molecular Weight ($kg/kgmole$)	670.80
Mass Density (kg/m^3)	997.98
Conradson Carbon ($wt\%$)	11.58
Mass Heat Capacity ($kJ/kgmole - K$)	2.784
Mass Heat of Vaporization (kJ/kg)	430.957
Surface Tension ($dyne/cm$)	27.046
Thermal Conductivity ($W/m - K$)	0.099
Viscosity (cP)	0.926

TABLE 4.2. Physical properties of gas

Gas	
Molecular Weight ($kg/kgmole$)	24.66
Mass Density (kg/m^3)	1.40
Mass Heat Capacity ($kJ/kgmole - K$)	3.645
Mass Heat of Vaporization (kJ/kg)	1984.244
Thermal Conductivity ($W/m - K$)	0.121
Viscosity (cP)	0.022

TABLE 4.3. Physical properties of distillates

Distillates	
Molecular Weight ($kg/kgmole$)	211
Mass Density (kg/m^3)	889.2
Mass Heat Capacity ($kJ/kgmole - K$)	2.822
Mass Heat of Vaporization (kJ/kg)	815.074
Thermal Conductivity ($W/m - K$)	0.046
Viscosity (cP)	0.015

Fig. 4.1 presents a comparison between the available properties reported in literature and the data obtained using Aspen Hysys. For the VRC molecular weight there is not much information reported in literature. According to the literature review, the molecular weight for VRC is between 810 and 1120 [18; 23], however the value obtained from Aspen Hysys is lower (670), as is shown in Fig. 4.1.a. For this case it is important to take into account that the crude properties depend on several factors that affect its composition, for this reason it is possible to obtain a crude with lower molecular weight compared to the founded data. For mass density, in literature are reported data from 900 to 1097 [17; 18; 38; 45; 46; 47; 48; 49], and the value obtained from Aspen Hysys is inside of this range (997) as is shown in Fig. 4.1.b. Finally, Fig. 4.1.c shows that a typical value for Conradson carbon were obtained (11.58) according to the range obtained from literature review ($9.1 - 25.5$) [17; 18; 22; 38; 45; 46; 47; 48; 49; 50].

To compare the values of molecular weight of the products, typical composition of gas and distillates were taken from [40; 51] respectively, to compute these properties through general rule of mixture. For gas, the molecular weight computed from literature was 28.71 and the obtained value from Aspen Hysys was 24.66, which is slightly lower than the computed value from literature. For distillates, the molecular weight calculated from [40] was 185.9 and the value obtained from Aspen Hysys was 211.0, which is slightly higher than the calculated value. It is important to remark that there is not much information about these properties in literature, for this reason only two references were used to validate these properties.

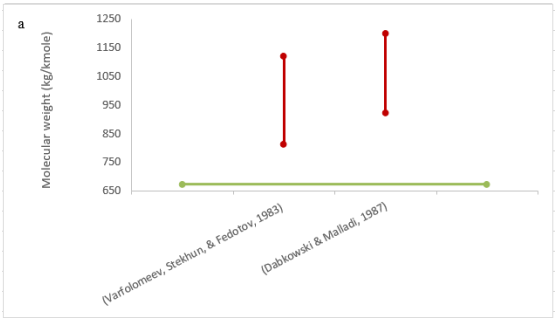

(a) VRC molecular weigh

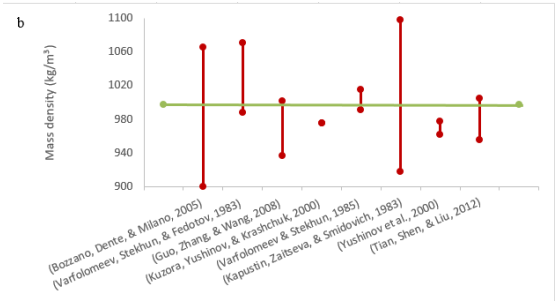

(b) VRC mass density

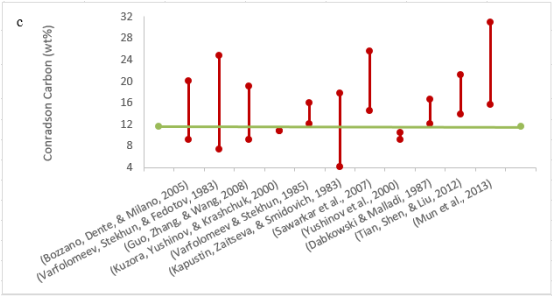

(c) VRC Conradson Carbon

FIGURE 4.1. Comparison between VRC properties according to literature (red) and VRC properties obtained using Aspen Hysys (green)

Additionally, as a result of the simulation the values for outlet temperature, mass flow at the outlet and yields were obtained. These results are presented in Table 4.4. The value for temperature is in the range of temperatures presented in Table 3.2 which summarizes the reported data in literature. The yields showed in Table 4.4 were validated with the data reported in [51].

TABLE 4.4. Results obtained from simulation using Delayed Coker Model

Outlet temperature (°C)	447
Outlet mass flow (kg/h)	124301.09
Gas $(wt\%)$	3.79
Coker Naphtha $(wt\%)$	10.58
Light Coker Gas Oil $(wt\%)$	21.11
Heavy Coker Gas Oil $(wt\%)$	31.76
Coke $(wt\%)$	32.52

To validate the product yields, a comparison with literature data was made as is shown in Fig. 4.2 according to [22; 49; 52; 53]. Fig. 4.2.a. shows the gas yields available in literature (red). According to literature data for gas yield, the result obtained from Aspen Hysys is slightly lower (green). Fig. 4.2.b. presents distillates yields from literature (red) and the result from Aspen hysys (green), which is in the range. Fig. 4.2.c. shows the yields of coke from literature (red) and the results from Aspen Hysys (green) which is in the range too.

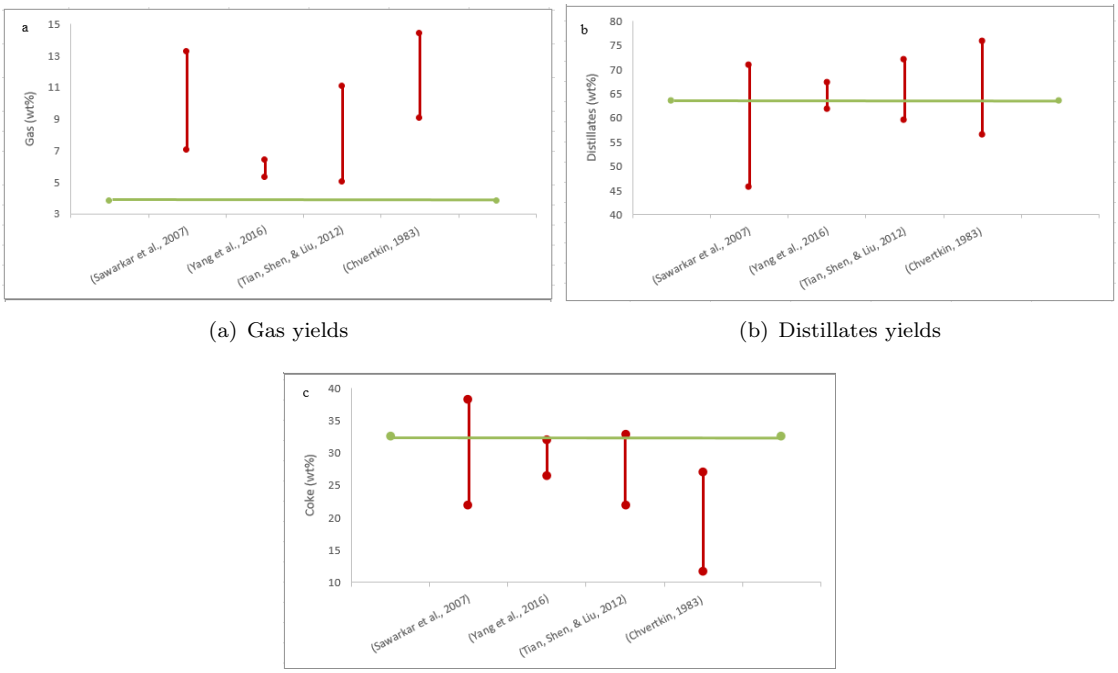

(a) Gas yields

(b) Distillates yields

(c) Coke yields

FIGURE 4.2. Comparison between product yields according to literature (red) product yields obtained using Aspen Hysys (green)

4.2. Selection of bottlenecks

According to literature review, the main bottlenecks in a coke drum could be formation of coke quality, hot spots and plugging and foamovers formation [3; 8; 23; 54; 55; 56; 57].

4.2.1. Coke quality

The quality of coke depends on four main characteristics: sulfur quantity, metals quantity, hardness and physical structure. The sulfur and metal content as well as the physical structure depends mainly on the feed to the reactor. On the other hand, hardness in coke is related to the quantity of volatile combustible material (VCM) in coke: high values of VCM is related to soft coke formation and low values of VCM is related to hard coke formation. The quantity of VCM could vary according to factors such as outlet temperature, pressure and time.

A soft coke tends to favor the formation of coked and partially coked particles, which could generate problems in the outlet. A hard coke generate problems in the cleaning stage because it is difficult to remove [3; 54; 56].

4.2.2. Hot spots

During the cleaning stage, the hot spots formed in the coke bed generate explosions, which could produce damage on the reactor surface [8; 54; 55].

4.2.3. Vapor line plug

Vapor line plug is the main problem in a DCU because it does not only affect the drum outlet but also generate further problems in other equipment of the unit. There are several undesired scenarios because of particle shift: coke formation in the outlet tube, partial or total plug of the bottoms of the fractionator tower due to a low quantity of coke and the coke formation inside the tubes of the furnace.

Other causes for vapor line plug is the coke formation by chemical reaction or by condensation. The use of some strategies could avoid the coking inside the outlet conduct, such as use of quench oil (LCGO, HCGO), entrance of the outlet conduct inside the reactor, modification of the outlet temperature, filled height control and in some cases, isolation of the outlet conduct [23; 54].

Table 4.5 shows a comparison between each bottleneck of the process, its relevance and the feasibility of using a CFD approach for its analysis. Taking into account the information of Table 4.5, the most important bottleneck and feasible for CFD simulation is the foamovers shift.

Table 4.5. Comparison between the main bottlenecks in the coke drum

Bottleneck	Relevance	Feasibility of the CFD use
Coke quality	**Medium relevance:** It could affect the coke drum operation and could difficult the cleaning stage	The coke quality mainly depends on the feed characteristics which is difficult to control using variations of the hydrodynamics
Hot spots	**Medium relevance:** There are some branches in the coke formation which are closed, it generates an accumulation of hydrocarbons in those zones. It could generate deformations of the drum wall because of possible explosions in the cleaning stage due to the air contact with hydrocarbons at high temperatures.	It is difficult to do a CFD simulation of the cleaning stage, moreover it is difficult to get data related to this stage.
Plugging of the vapor line	**High relevance:** It could affect the reactor operation and the operation of other equipment due to the shift of particles.	It is possible to analyze the coke formation at the top of the reaction taking into account the possible chemical reactions of the process

4.3. Possible routes of plugging on the vapor line wall

According to Section 2.3, the possibles routes for the coke formation are: coke formation by chemical reaction, condensation of high boiling point components and mechanical deposition. Fig. 4.3 outlines the possible routes for coke formation in the vapor line for a coke drum. In the next subsections the results of the evaluation of each route are shown.

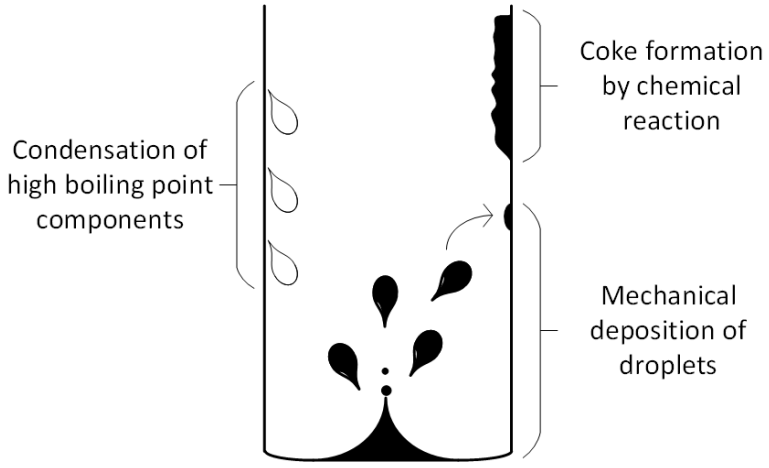

FIGURE 4.3. Possible routes for coke formation

4.3.1. Vapor line plugging by condensation

The thermodynamic state of the components into the reactor was evaluated at different conditions of pressure and temperature. To obtain that information Aspen - Hysys was used. According to the information showed in Section 3.2, the thermodynamic state of the components were evaluated in a pressure range between $35-700$ kPa and in a temperature range between $415-482$ °C.

Considering that the inlet temperature could affect the composition of the products, a variation of the inlet temperature in the Delayed Coker Model was made. Eight scenarios were considered in which the inlet temperature varies into the proposed range in Section 3.2 ($450-515$ °C). For each case, a evaluation of the thermodynamic state was made to study the possibility of coke formation by condensation of high boiling point components route. For each scenario the pressure was established as 200 kPa.

In a first scenario the outlet temperature obtained from the Delayed Coker Model were 401 °C. For these conditions and for the current composition of the products, the liquid fraction is 0.0073. In Fig 4.4 the evaluation of the liquid fraction presence at several values of temperature and pressure for the current composition is shown.

The evaluation was made for eight scenarios in a range of temperatures between $450-515$ °C and considering the typical operational pressure is 200 kPa and Assuming that all liquid fraction is converted in coke. Table 4.6 summarizes the results for all scenarios.

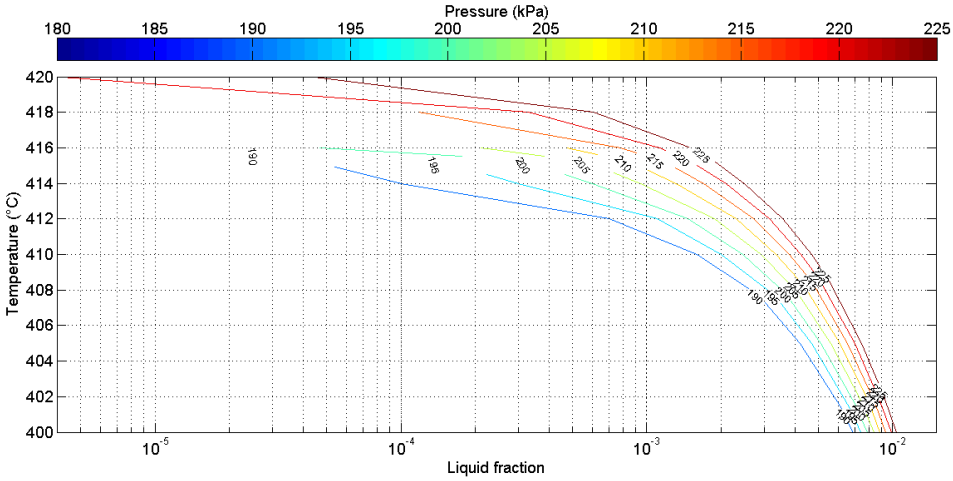

FIGURE 4.4. Liquid fraction at different temperatures (y-axis from 400 - 420 °C) and pressures (colorbar from 180 - 225 kPa)

TABLE 4.6. Liquid fractions at 200 kPa and at different temperatures

Inlet temperature °C	**Outlet temperature °C**	**Liquid fraction**
450	401	0.0073
460	410.6	0.0026
470	420.6	0
480	430.6	0
490	422	0
500	425.5	0
510	463.7	0
515	469	0

The most common operational temperature is around 500 °C and at this temperature there is not presence of liquid. Moreover, according to Table 4.6, there is liquid only in ranges of temperature between $450 - 460$ °C but the quantities are not significant.

4.3.2. Surface velocity for coke reaction

The current reaction velocity has volume units, however for the case of study it is important to have a surface reaction velocity. To obtain a surface reaction velocity it is necessary to obtain a characteristic length to transform the volumetric reaction velocity into a surface one. An analysis from $y+$ definition was made to calculate that characteristic length.

$y+$ definition: Dimensionless length

$$y+ = \frac{\rho y v*}{\mu} \tag{4.1}$$

where $v*$ is defined as follows

$$v* = \sqrt{\frac{\tau_w}{\rho}} \tag{4.2}$$

From Eq. 4.1 we can obtain the value of y

$$y = \frac{\mu y+}{\rho v*} \tag{4.3}$$

$y+$ does not affect the dimension of the equation, so we can define a new value for y

$$y_2 = \frac{5\mu}{\rho v*} \tag{4.4}$$

Then to obtain a surface reaction velocity the Eq. 4.5 is used.

$$r_{surf} = y_2 r_{vol} \tag{4.5}$$

Considering the kinetic parameters presented in Table 3.5, the contours for the volumetric rate of coke reaction is shown in Fig. 4.5. In the vapor line, the order of magnitude of the volumetric rate of coke reaction is around 1.9×10^{-8} $mol/m^3 s$, according to Fig. 4.5. The small value of the volumetric rate of coke reaction is because to the low concentration of VRC at the top of the reactor.

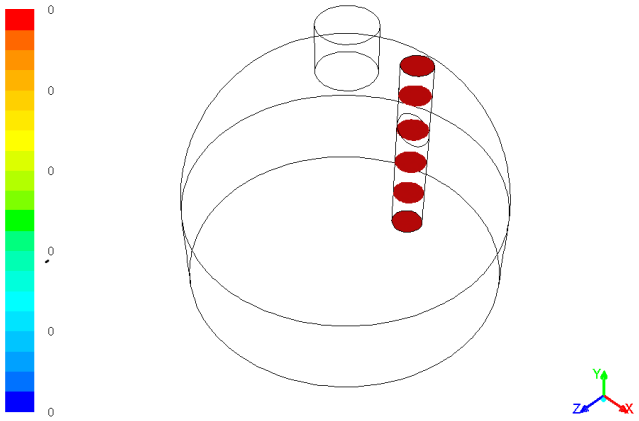

FIGURE 4.5. Contours of volumetric rate of coke reaction in the vapor line

Fig. 4.6 shows the values of the characteristic length y_2 using Eq. 4.4. The order of magnitude of this values is $1 \times 10^{-7}\ m$. These values are small and considering the small values of the volumetric rate of coke reaction, using Eq. 4.5, the values of the surface rate will be even smaller, as is shown in Fig. 4.7.The values for r_{surf} are around 1×10^{-12} mol/m^2s which are almost zero, which means that there is no coke deposition by chemical reaction.

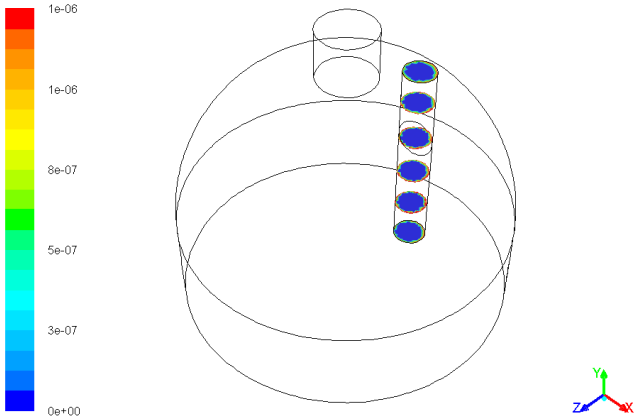

FIGURE 4.6. Contours for values of y_2

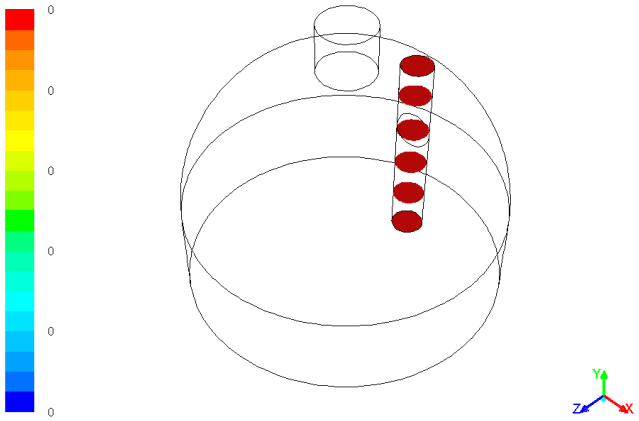

FIGURE 4.7. Surface reaction rate

4.3.3. Vapor line plugging by mechanical deposition of particles

Mechanical deposition of coke due to heavy hydrocarbon droplet-wall interaction has been evaluated before for convection section of steam crackers [13; 58]. According to this and the selected bottleneck, the shift of particles was evaluated to verify the vapor line

plug because of it. For this case, a CFD simulation was carried out to compute possible trajectories of the particles and verify if some of them can stick in the vapor line.

The behavior of impinging droplets depend on wall temperature and the Weber's number. The Weber's number is a dimensionless number which relates the importance between inertial forces of the fluid and its surface tension. The Weber's number is defined as:

$$We = \frac{\rho v^2 D_d}{\gamma} \tag{4.6}$$

Where D_d is the diameter of the droplet, ρ is the fluid density, v is the fluid velocity and γ is the surface tension of the fluid.

S. De Schepper et al.[13] assume that heavy hydrocarbon droplets behavior is similar to the behavior of diesel droplets. Taking this into account, there are three possible droplet behavior when it impinging the wall: stick, rebound and splash. If Weber's number is above 80 the droplet splashes, if the Weber's number is under 80 and the wall temperature is under boiling temperature of the fluid the droplet sticks and if the Weber's number is under 80 and the wall temperature is above boiling temperature of the fluid the droplet rebounds. For the case of VRC the wall temperature was considered as the outlet temperature (440 °C) taken from the base case of the Delayed Coker Model from Aspen Hysys, as well as VRC density, velocity and surface tension at the same temperature. Considering a distillation curve for VRC Fig. 4.8, the wall temperature is always under VRC boiling point. The possible behavior of the droplet is shown in Fig. 4.9.

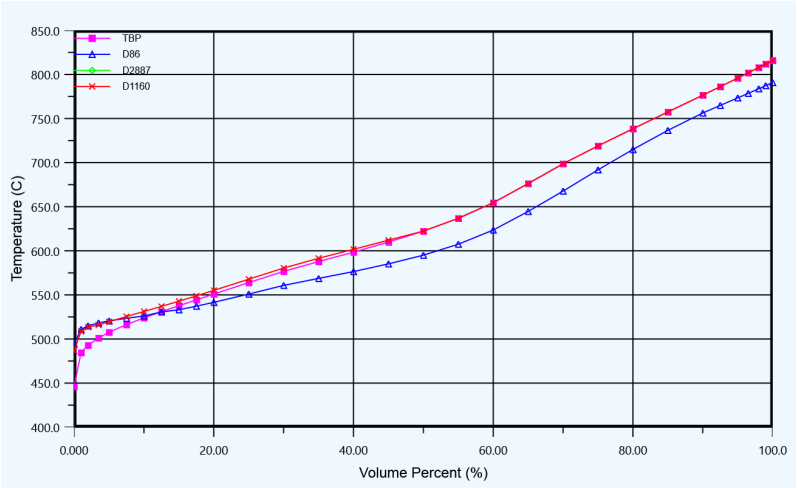

FIGURE 4.8. Distillation curves for VRC

The Weber's number was computed for several droplet diameters and for most of the cases the droplet sticks (Table 4.7). The particle diameter required for the splash of the droplet is around 43 *cm*. For this case of study, the main assumption is that droplets form from bursting bubbles, thus droplet diameters of 43 *cm* are not reasonable.

For the evaluation of the droplets diameters the bursting bubble methodology proposed in section 3.6 was employed.

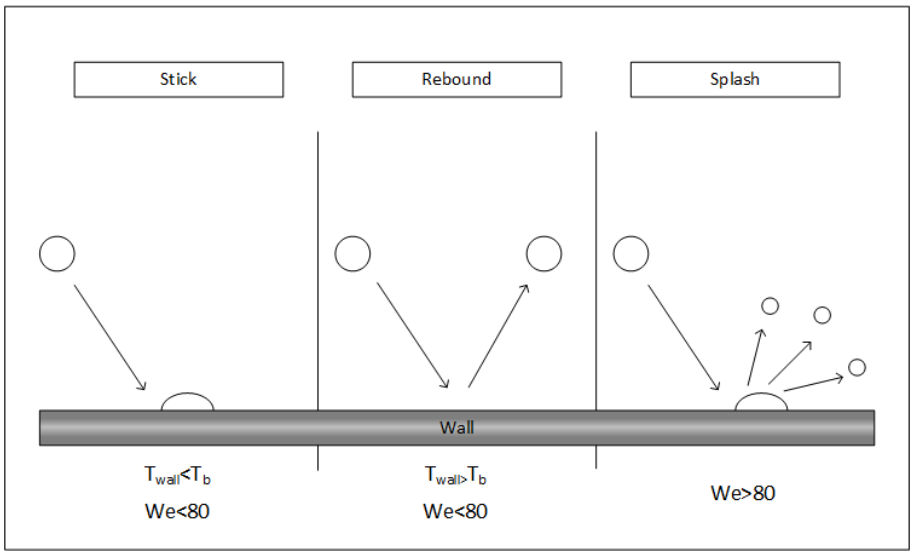

FIGURE 4.9. Droplets behavior according to the Weber's number and wall temperature

TABLE 4.7. Weber's number at six different droplet diameters

Droplet diameter (m)	**Weber's number**	**Droplet behavior**
5×10^{-6}	9.260×10^{-3}	Stick
5×10^{-5}	9.260×10^{-2}	Stick
5×10^{-4}	9.260×10^{-1}	Stick
5×10^{-3}	9.260×10^{0}	Stick
4.3×10^{-2}	7.963×10^{1}	Stick
5×10^{-2}	9.260×10^{1}	Splash

To compute the possible drop diameters it is important to know the film foll-up speed S_f and the film thickness h which varies between 0.3 and 3 μm. According to the values of S_f, some possible droplet diameters (D_d) can be obtained using Eq. 3.13. According to the values of S_f, some possible bubble diameters (D_d) can be obtained. Table. 4.8 shows the values of D_d and S_f at different values of h.

TABLE 4.8. Droplet diameters at different roll-up speeds and bubble thickness

h (m)	3.0×10^{-7}	5.0×10^{-7}	1.0×10^{-6}	1.5×10^{-6}	2.0×10^{-6}	2.5×10^{-6}	3.0×10^{-6}
S_f (mm)	2.6×10^{0}	3.5×10^{0}	4.7×10^{0}	5.4×10^{0}	5.9×10^{0}	6.3×10^{0}	6.6×10^{0}
D_d (μm)	2.4×10^{1}	3.1×10^{1}	4.3×10^{1}	5.3×10^{1}	6.1×10^{1}	6.8×10^{1}	7.5×10^{1}

4.3.3.1. CFD simulation

Mesh independence

To carry out a CFD simulation, it is necessary to develop a mesh independence, it is to guarantee that change in mesh does not affect the results of the simulation. For this, two cases for mesh independence were evaluated, first in the cylinder zone and later in the vapor line. The number of cells used for the simulation was around 950000 and the mesh independence were evaluated for cell numbers near to this value to verify that around this value there is not significant changes.

Fig. 4.10, shows four different planes in the geometry where the average velocity were evaluated (left) and the velocity values for each position (right) evaluated for five different meshing. According to Fig. 4.10, there are not significant differences between the evaluated mesh.

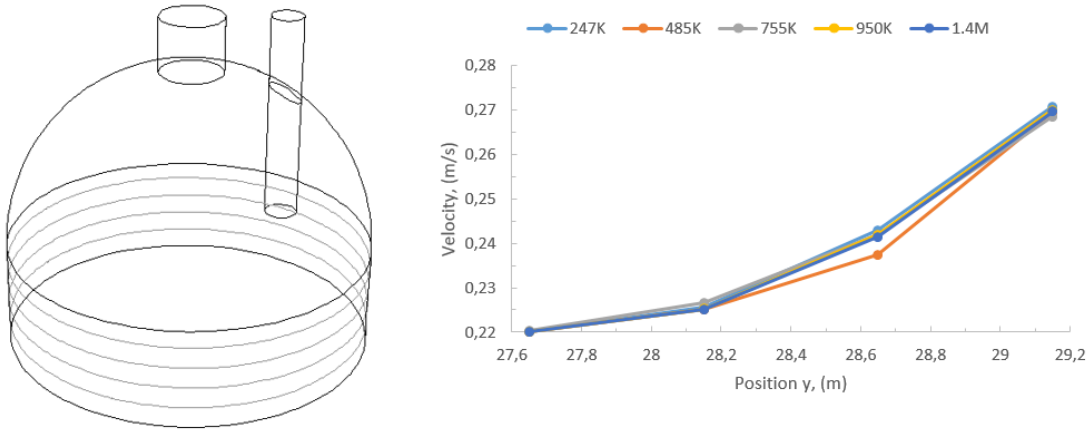

FIGURE 4.10. Mesh independence in cylinder section

Fig. 4.11, shows then different planes in the geometry in the vapor line zone where the average velocity were evaluated (left) and the velocity values for each position (right) evaluated for five different meshing. According to Fig. 4.11, there are not significant differences between the evaluated mesh.

Base case: tube at level with the reactor's surface

Fig. 4.12 shows the trajectory of the injected particles (4275 injected particles), where the color bar represents the residence time of the particles. The mean residence time is around of 24.2 s but almost all the particles go out of the reactor. According to the simulation, the percentage of injected particles deposited is 5.54%. Fig. 4.13 presents the contours of DPM accretion rate. The deposited particles are mainly at the bottom of the tube and the accretion rate is around $1.03 \times 10^{-3}\ kg/m^2 s$.

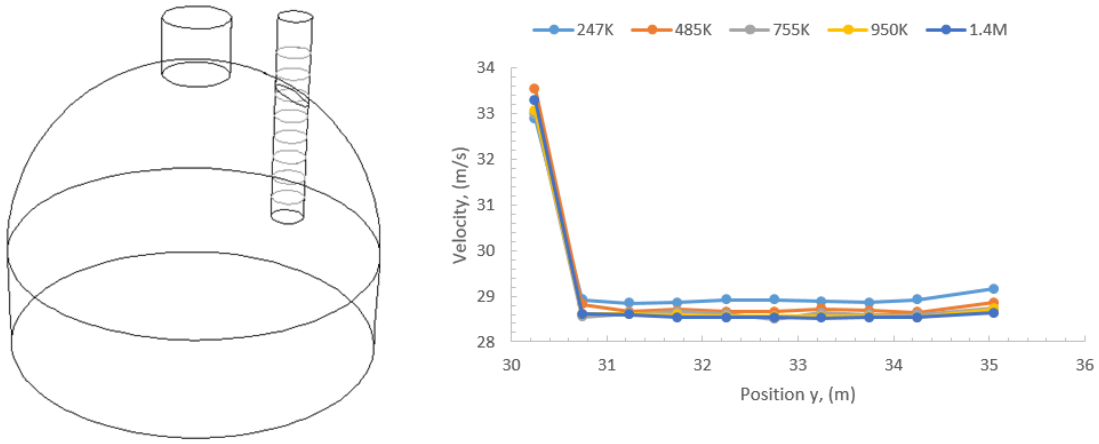

FIGURE 4.11. Mesh independence in vapor line section

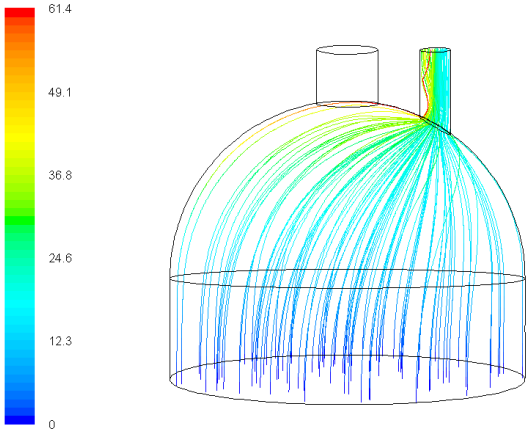

FIGURE 4.12. Trajectory base case: tube at level with the reactor's surface

Vapor line modifications

Three cases have been taken into account for the evaluation of the accretion of the particles. J. Roth [59] shows that is possible to reduce the fouling of the vapor line introducing a part of the tube into the reactor. It makes sense because if the tube does not enter in the drum a funnel-effect can increase the particle shift.

An evaluation of the model was made using the maximum value of the droplet diameter, according to Table 4.8. Three cases have been taken into account for the evaluation of the deposition of the droplets: a base case where there is tube at level with the reactor's surface, tube of 30 cm into the reactor and a tube of 3 m into the reactor. The base case was explained before.

a) 30 cm ***tube into the reactor***: Fig. 4.14 shows the trajectory of the injected particles (4510 injected particles), where the color bar represents the residence time of the particles. The mean residence time is around of 23.9 s. According to the simulation,

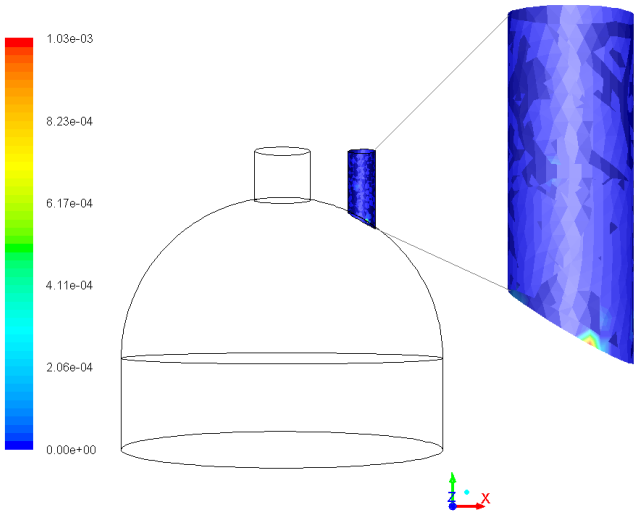

FIGURE 4.13. Deposition rate of particles for Base case: tube at level with the reactor's surface

the percentage of injected particles deposited is 2.22%. Fig. 4.15 presents the contours of DPM accretion rate. The deposited particles are mainly at the bottom of the tube and the accretion rate is around 9.333×10^{-5} kg/m^2s.

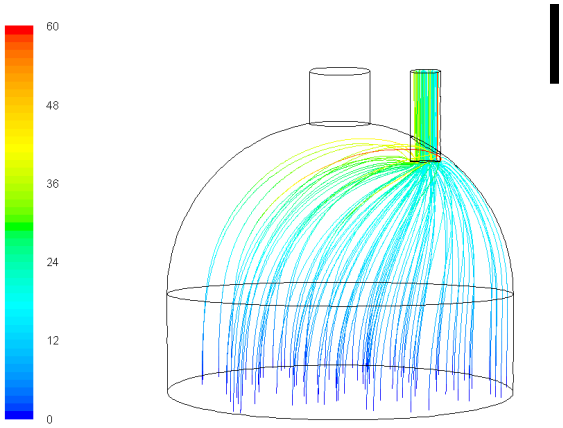

FIGURE 4.14. Trajectory of the particles for a 30 cm entered tube

b) 3 m ***tube into the reactor***: Fig. 4.16 shows the trajectory of the injected particles (5412 injected particles), where the color bar represents the residence time of the particles. The mean residence time is around of 24.2 s but all the particles go out of the reactor. According to the simulation, the percentage of injected particles deposited is 1.50%. Fig. 4.17 presents the contours of DPM accretion rate. The deposited particles are mainly at the bottom of the tube and the accretion rate is around 6.41×10^{-5} kg/m^2s.

According to Fig. 4.14 and 4.16, the change in vapor line length increase the residence time at the top of the reactor which difficult the outlet of particles.

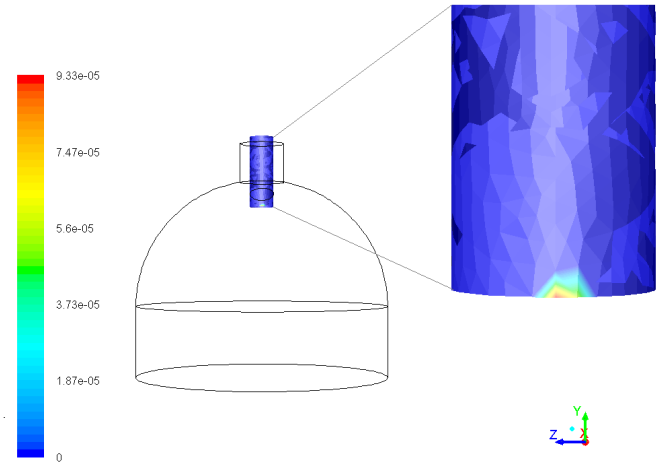

FIGURE 4.15. Deposition rate of particles for 30 cm entered tube

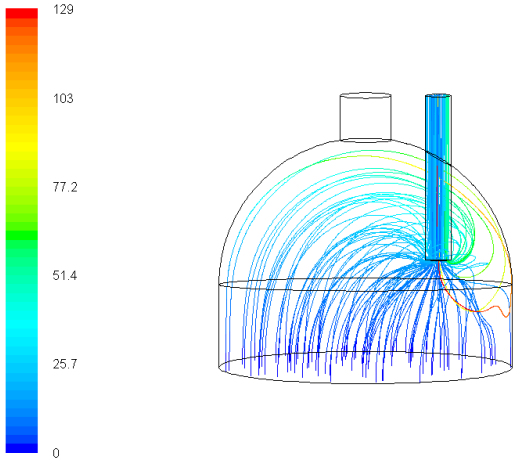

FIGURE 4.16. Trajectory of the particles for a 3 m entered tube

Considering the maximum value of the accretion rate for each case, the thickness of the deposition was computed. For the first case, in a month the thickness of coke in the affected zone is around of 1.67 m.

Similar to the first case, the maximum value of the accretion rate was considered to compute the thickness at different values of times. The thickness of the deposition in a month is around of 90 cm. Comparing with the Base case: tube at level with the reactor's surface case, the thickness reduction of coke is considerable.

For the last case, the maximum value of the accretion was used to compute the thickness at different times as well. The thickness of the deposition in a month is around of 62.3 cm.

To do a properly comparison between cases, a plug percentage were computed. According to the plug percentages for each case considering the tube diameter (1.75 m). The maximum percentages for each case are 95.3, 8.6 and 5.9 respectively. The difference between

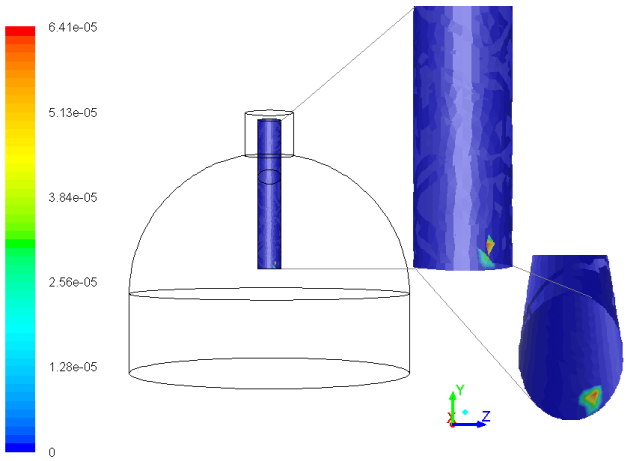

FIGURE 4.17. Deposition rate of particles for a 3 m entered tube

the first case and second case is significantly larger (86.7%) in comparison to the difference between the second case and the third case (2.7%). Considering the magnitude order difference between the second case and the third case, the percentage difference is not too larger thus, the second option is considered a better option.

Table 4.9 summarizes the results for three cases mentioned above for different values of days: 1, 7, 14 and 30 days.

Geometry modification

To evaluate a possible improvement of the above results, a geometry modification is proposed. Fig. 4.18 shows a modification at the top of the cylinder, increasing the cross area to reduce the particle velocity. For the evaluation of the new geometry effect a change of diameter of 16%.

A CFD simulation was carried out to evaluate if the change of the geometry could reduce the deposition on the vapor line wall. The length of the vapor line into the reactor evaluated for the three cases mentioned above.

a) ***Tube at level with the reactor's surface***: Fig. 4.19 shows the trajectory of the injected particles for the new geometry and considering tube at level with the reactor's surface (3802 injected particles), where the color bar represents the residence time of the particles. The mean residence time is around of 54.8 s. According to the simulation, the percentage of injected particles deposited is 5.79%. Fig. 4.20 presents the contours of DPM accretion rate. The deposited particles are mainly at the bottom of the tube and the accretion rate is around $1.24 \times 10^{-3}\ kg/m^2 s$.

b) 30 cm ***tube into the reactor***: Fig. 4.21 shows the trajectory of the injected particles for the new geometry (3802 injected particles), where the color bar represents the residence time of the particles. The mean residence time is around of 53.5 s. According to the simulation, the percentage of injected particles deposited is 2.31%. Fig. 4.22

TABLE 4.9. Summary of different cases for entered tube: tube at level with the reactor's surface, 30 cm entered tube and 3 m entered tube

Tube at level with the reactor's surface		
Accretion Rate (kg/m^2s):	1.03×10^{-3}	
Time (d)	**Thickness (m)**	**Plug (%)**
1	5.56×10^{-2}	3.2
7	3.89×10^{-1}	22.2
14	7.79×10^{-1}	44.5
30	1.67×10^{0}	95.3
30 cm Entered tube		
Accretion Rate (kg/m^2s):	9.33×10^{-5}	
1	5.04×10^{-3}	0.3
7	3.53×10^{-2}	2.0
14	7.05×10^{-2}	4.0
30	1.51×10^{-1}	8.6
3 m Entered tube		
Accretion Rate (kg/m^2s):	6.41×10^{-5}	
1	3.46×10^{-3}	0.2
7	2.42×10^{-2}	1.4
14	4.85×10^{-2}	2.8
30	1.04×10^{-1}	5.9

presents the contours of DPM accretion rate. The deposited particles are mainly at the bottom of the tube and the accretion rate is around 8.23×10^{-4} kg/m^2s.

c) 3 m ***tube into the reactor***: Fig. 4.23 shows the trajectory of the injected particles for the new geometry (3802 injected particles), where the color bar represents the residence time of the particles. The mean residence time is around of 54.9 s. According to the simulation, the percentage of injected particles deposited is 1.60%. Fig. 4.24 presents the contours of DPM accretion rate. The deposited particles are mainly at the bottom of the tube and the accretion rate is around 1.25×10^{-4} kg/m^2s.

According to the results obtained from the change of the geometry, it is recommended do not change the geometry because the particles reduce their velocity and increase the residence time in the middle of the reactor which ease the entrance of particles to the vapor line and it increases the deposition of particles. However, similar to the case with no geometry modifications, the number of particles inside of the vapor line decrease with the increase of the tube length.

Table 4.10 summarizes the results for three cases mentioned above for different values of 25days: 1, 7, 14 and 25 days.

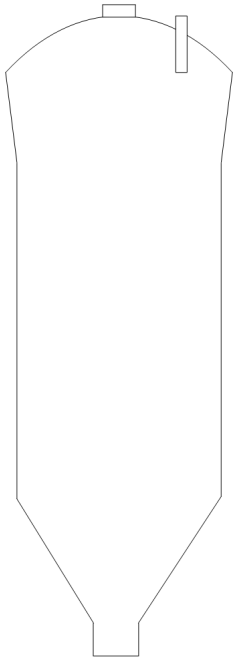

FIGURE 4.18. Coke drum with variable diameter

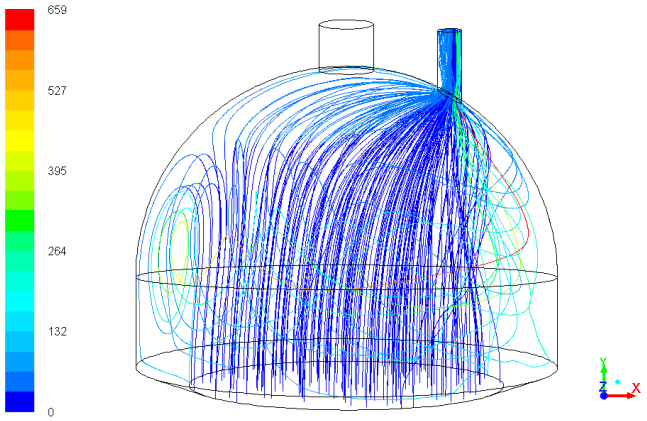

FIGURE 4.19. Trajectory of the particles for tube at level with the reactor's surface in a coke drum with variable diameter

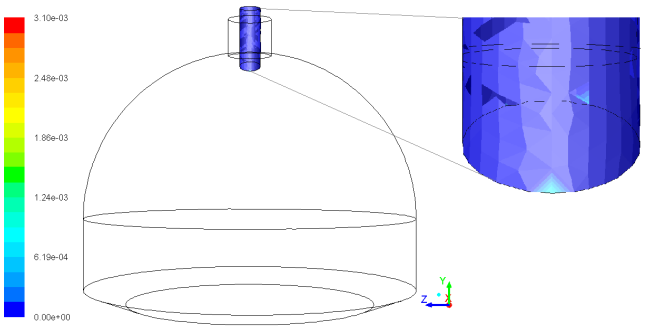

FIGURE 4.20. Accretion rate of particles for Base case: tube at level with the reactor's surface

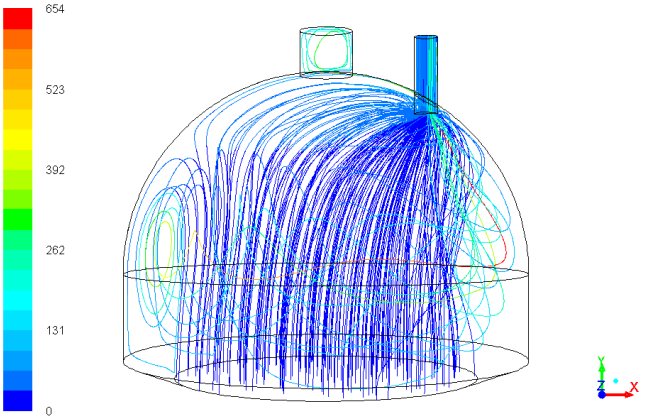

FIGURE 4.21. Trajectory of the particles for a 30 *cm* entered tube in a coke drum with variable diameter

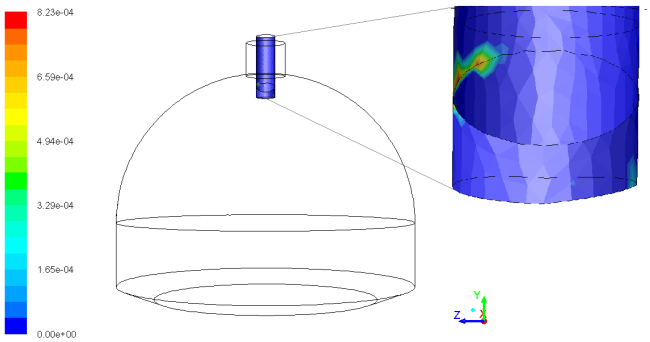

FIGURE 4.22. Accretion rate of particles for 30 cm entered tube in a coke drum with variable diameter

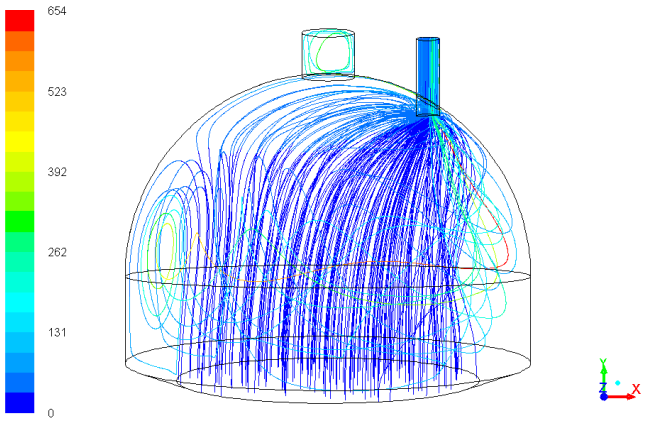

FIGURE 4.23. Trajectory of the particles for a 3 m entered tube in a coke drum with variable diameter

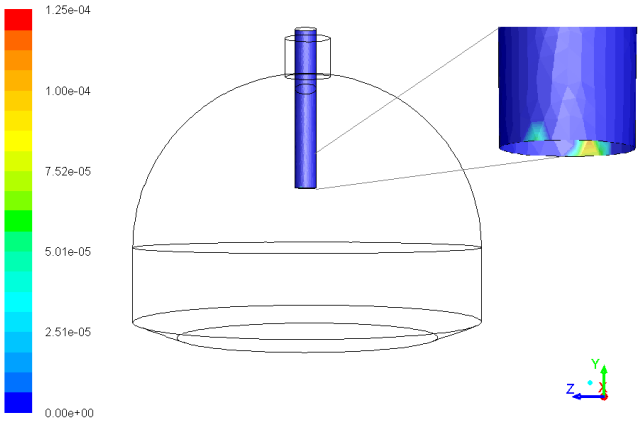

FIGURE 4.24. Accretion rate of particles for 3 m entered tube in a coke drum with variable diameter

TABLE 4.10. Summary of different cases for entered tube: tube at level with the reactor's surface, 30 cm entered tube and 3 m entered tube for a new geometry

Tube at level with the reactor's surface		
Accretion Rate (kg/m^2s)**:**	$1..24\times10^{-3}$	
Time (d)	**Thickness** (m)	**Plug** (%)
1	6.70×10^{-2}	3.8
7	4.69×10^{-1}	26.8
14	9.37×10^{-1}	53.6
25	1.67×10^{0}	95.7
30 cm Entered tube		
Accretion Rate (kg/m^2s)**:**	9.33×10^{-5}	
1	4.44×10^{-2}	2.5
7	3.11×10^{-1}	17.8
14	6.22×10^{-1}	35.6
25	1.11×10^{-0}	63.5
3 m Entered tube		
Accretion Rate (kg/m^2s)**:**	6.41×10^{-5}	
1	6.75×10^{-3}	0.4
7	4.73×10^{-2}	2.7
14	9.45×10^{-2}	5.4
25	1.69×10^{-1}	9.64

Conclusions

This thesis presents a review of the operational parameters of a delayed coking unit as well as the possible inefficiencies of the process, particularly in the reactor. There are several problems in the delayed coking process, however the most important are hot spots, quality of coke and plugging of the vapor line by coke formation.

To do a CFD simulation, it is important to know some properties of the process components, for this reason a simulation using the Delayed Coker Model from Aspen Hysys was made. Some properties obtained using the Delayed Coker Model were validated using reported values in literature. According to it, the values for VRC molecular weight is lower than the literature reported data. However, there are not much information about it in literature and it is possible that the characterized crude was lighter than the crude reported in literature. Another value that is slightly lower than reported data is the gas yield, but it is important to remark that the dalayed coking process depends strongly on the operational conditions and the feed, which can affect significantly the product yields.

The selected bottleneck was the plugging of the vapor line by coke formation because it does not affect only the reactor. The semi-coked particles could be shifted to other units of the process.

The possible routes for coke formation on the vapor line wall are condensation of heavy components, chemical reaction of the remaining feed fraction and plugging by mechanical deposition.

The analysis of the condensation of heavier components of the outlet, presented that the possibility of the coke formation by this route is reduced.

The analysis of the surface chemical reaction shows that the deposition by chemical reaction is not feasible because of the low concentration of VRC at the outlet which implies that the rate of coke production is technically zero.

Considering that all the particles are reflected at the reactor walls, most of the particles could be taken to the other equipment of the unit. On the other hand, according to the accretion model employed, there is possible the particle deposition at the bottom of the vapor line by this route, considering the condition of "trap" into the tube.

The changes in the length of the vapor line could affect the deposition of coke: grater length implies less deposition of coke. However there is a length from the reduction of the deposition is not significant.

A change of the drum geometry was proposed to evaluate a possible reduction of the coke deposition in the vapor line. However, to increase the volume of the drum at the top causes

a long residence time of the semi-coked particles at the top which increase the deposition of coke in the vapor line for the two evaluated cases (30 cm and 3 m entered tube).

Future Work

After completing this work, the following aspects must be revised or explored towards complementing the outcome of this thesis:

- Validate the results of the simulations with experimental information.
- Look for tools for the improvement of the yields of the valuable products of the process.
- Evaluate possible changes in operational parameters to avoid the coke formation at the vapor line without affect the yields of valuable products.
- Try different geometry alternatives to avoid the plugging of the vapor line taking into account not only the top of the reactor but the whole reactor.

References

[1] Luis Carlos López. Kinetic mechanism for the cracking of Colombian heavy crude oil fractions in refinery equipments Kinetic mechanism for the cracking of Colombian heavy crude oil fractions in refinery equipments, 2015.

[2] UPME. Escenarios de Oferta y Demanda de Hidrocarburos en Colombia. Technical report, Bogotá D.C., 2012.

[3] Fabian Andrey Diaz-Mateus. Desarrollo de un Modelo de Simulación para el Proceso de Coquizacion Retardada de Residuos de la Refinacion de Crudos Colombianos. 2013.

[4] ECOPETROL. Refinería de Barrancabermeja 2011 - 2015: Plan de "conversión" y modernización, 2011. URL `http://www.ecopetrol.com.co/especiales/carta{_}petrolera125/refinacion.htm`.

[5] G G Valyavin, E A Khukhrin, and K G Valyavin. The place of delayed coking in modern oil rerineries. *Chemistry and Technology of Fuels and Oils*, 43(3):15–18, 2007.

[6] Muhammad Syukri Bin Mohd Shah and Balasubramanian Periyasamy. Binary cracking kinetics for thermal cracking of vacuum residues in Eureka process. *Fuel*, 134: 618–627, 2014. ISSN 00162361. doi: 10.1016/j.fuel.2014.06.021.

[7] Q Chen. Energy-use analysis and improvement for delayed coking units. *Energy*, 29 (12-15):2225–2237, dec 2004. ISSN 03605442. doi: 10.1016/j.energy.2004.03.021.

[8] Paul J Ellis, Christopher A Paul, and Port Arthur. Tutorial : Delayed Coking Fundamentals. *AIChE 1998 Spring National Meeting*, pages 1–20, 1998.

[9] Yang Lei, Bingjian Zhang, Xiaoqiong Hou, and Qinglin Chen. A Novel Strategy for Simulating the Main Fractionator of Delayed Cokers by Separating the Desuperheating Process. *Chinese Journal of Chemical Engineering*, 21(3):285–294, mar 2013. ISSN 10049541. doi: 10.1016/S1004-9541(13)60472-4.

[10] Hessam Vakilalroayaei, Mazda Biglari, Ali Elkamel, and Ali Lohi. Dynamic behavior of coke drum process safety valves during blocked outlet condition in the refinery delayed coking unit. *Journal of Loss Prevention in the Process Industries*, 25(2): 336–343, mar 2012. ISSN 09504230. doi: 10.1016/j.jlp.2011.12.002.

[11] F Rodriguez-Reinoso, P Santana, E Romero Palazon, M-A Diez, and H Marsh. Delayed coking: industrial and laboratory aspects. *Carbon*, 36(97):105–116, 1998.

[12] L V Meléndez, R Cabanzo, E Mejía-Ospino, and A Guzmán. Physico-chemical characterization of products from vacuum oil under delayed coking process by infrared spectroscopy and chemometrics methods Self-organization experimentally modeled by chemometrics and data-inspection emphasizes the strength of an explora. *J. Phys.: Conf. Ser*, 687, 2016.

[13] Sandra C K De Schepper, Geraldine J. Heynderickx, and Guy B. Marin. Modeling the coke formation in the convection section tubes of a steam cracker. *Industrial and Engineering Chemistry Research*, 49(12):5752–5764, 2010. ISSN 08885885. doi: 10.1021/ie100091e.

[14] John D Elliot. Delayed Coking - Innovations and Trends. *Chemistry and Technology of Fuels and Oils*, 31(2):9–17, 1995.

[15] Tim Olsen. An Oil Refinery Walk - Trhough. *Chemical Engineering Process*, pages 34–40, 2014.

[16] Reza Sadeghbeigi. *Fluid Catalytic Cracking Handbook. An expert Guide to the Practical Operation, Design and Optimization of FCC Units*. 2012. ISBN 9780123869654.

[17] Giulia Bozzano, Mario Dente, and Politecnico Milano. A Mechanistic Approach to Delayed Coking Modelling. *European Symposium on Computer Aided Process Engineering*, pages 529–534, 2005.

[18] D F Varfolomeev, A I Stekhun, and V E Fedotov. Effect of Pressure on Coke Yield in Delayed Coking. *Chemistry and Technology of Fuels and Oils*, (12):26–28, 1983.

[19] Baoshi Wang, Jianhua Zhu, Longyan Wang, Ruyi Qin, and Xiaomin Chen. Experimental investigation of secondary reactions of intermediates in delayed coking. *Research on Chemical Intermediates*, 38(9):2295–2307, apr 2012. ISSN 0922-6168. doi: 10.1007/s11164-012-0546-5.

[20] Mohamed A. Fahim, Taher A. Al-Sahhaf, and Amal Elkilani. *Fundamentals of Petroleum Refining*, volume 19. Elsevier, 2009. ISBN 0080931561.

[21] Mario Dente, Giulia Bozzano, and Tiziano Faravelli. Kinetic modeling of pyrolysis processes in gas and condensed phase. In Guy B. Marin, editor, *Advances in Chemical Engineering*, pages 52–161. Academic Press, 2007. ISBN 0080545874.

[22] A. N Sawarkar, A Pandit, and J Joshi. Studies in Coking of Arabian Mix Vacuum Residue. *Chemical Engineering Research and Design*, 85(4):481–491, jan 2007. ISSN 02638762. doi: 10.1205/cherd06159.

[23] Michael J. Dabkowski and Madhava Malladi. Delayed coking process, 1987.

[24] H. Cai, a. Krzywicki, and M. C. Oballa. Coke formation in steam crackers for ethylene production. *Chemical Engineering and Processing*, 41(3):199–214, 2002. ISSN 02552701. doi: 10.1016/S0255-2701(01)00135-0.

[25] Lyle F Albright and James C Marek. Mechanistic model for formation of coke in pyrolysis units producing ethylene. *Industrial & Engineering Chemistry Research*, 27 (5):755–759, 1988. ISSN 08885885. doi: 10.1021/ie00077a006.

[26] Lyle F. Albright and James C. Marek. Coke formation during pyrolysis: roles of residence time, reactor geometry, and time of operation. *Industrial & Engineering Chemistry Research*, 27(5):743–751, 1988. ISSN 0888-5885. doi: 10.1021/ie00077a004.

[27] M. J. Bennet and J. B. Price. A Physical and Chemical Examination of an Ethylene Steam Cracker Coke and the Underlying Pyrolisis Tube.pdf. *Journal of Material Science*, 16, 1981.

[28] Edd Anders Blekkan and Anders Holmen. Coke formation on metal foils from heavy oils. *Carbon*, 25(6):827–835, 1987. ISSN 00086223. doi: 10.1016/0008-6223(87)90158-8.

[29] F.D. Kopinke, G. Zimmermann, and S. Nowak. On the mechanism of coke formation in steam cracking-conclusions from results obtained by tracer experiments. *Carbon*, 26(2):117–124, 1988. ISSN 00086223. doi: 10.1016/0008-6223(88)90027-9.

[30] A. Mohamadalizadeh, J. Towfighi, and R. Karimzadeh. Modeling of catalytic coke formation in thermal cracking reactors. *Journal of Analytical and Applied Pyrolysis*, 82(1):134–139, 2008. ISSN 01652370. doi: 10.1016/j.jaap.2008.02.006.

[31] Geert C Reyniers, Gilbert F Froment, Frank-Dieter Kopinke, and Gerhard Zimmermann. Coke Formation in the Thermal Cracking of Hydrocarbons. 4. Modeling of Coke Formation in Naphtha Cracking. *Industrial & Engineering Chemistry Research*, 33(11):2584–2590, 1994. ISSN 0888-5885. doi: 10.1021/ie00035a009.

[32] Paul J Ellis and Edward E Hardin. How petroleum delayed coke forms in a drum. *Light Metals*, pages 509 – 515, 1993.

[33] X.-L. Zhou, S.-Z. Chen, and C.-L. Li. A Predictive Kinetic Model for Delayed Coking. *Petroleum Science and Technology*, 25(12):1539–1548, dec 2007. ISSN 1091-6466. doi: 10.1080/10916460500529001.

[34] A Del Bianco, N Panariti, M Anelli, P. L Beltrame, and P Carniti. Thermal cracking of petroleum residues: 1 . Kinetic analysis of the reaction. *Fuel*, 72:75–80, 1993.

[35] Refa Köseoglu and Colin Phillips. Kinetics model for the non-catalytic hydrocracking of Athabasca bitumen. *Fuel*, 67:906–915, 1987.

[36] L. Mendonça Filho. *Modelagem e Simulaçao de Reator Trifásico Aplicado a Óleos Pesados com Reaçoes de Hidrocraqueamento Térmico e Catalítico, Demetalizaçao Deposiçao de Coque na Mistura e no Catalisador*. PhD thesis, UNICAMP, Campinas-SP, Brazil, 1998.

[37] John D. Elliot. Desing, operation factors can up coker liquid yields. *Oil & Gas Journal*, 1991.

[38] S M Kapustin, N P Zaitseva, and E V Smidovich. Role of Recycle Ratio in Delayed Coking Process. *Chemistry and Technology of Fuels and Oils*, (12):28–29, 1983.

[39] Masaaki Oka, Himsar Ambarita, Masashi Daimaruya, and Hiroyuki Fujiki. Study on the Effects of Switching Temperature on the Thermal Fatigue Life of the Shell-to-Skirt Junction of Coke Drum. *Journal of Pressure Vessel Technology*, 133(6):061210, 2011. ISSN 00949930. doi: 10.1115/1.4004564.

[40] Juan Esteban Torres-Macías. Inquietud sobre el proceso de coquización lenta. [email]. Technical report, Ecopetrol, 2014.

[41] Caleigh Holden. Jump Start : Delayed Coker Model in Aspen HYSYS ® Petroleum Refining. Technical report, Aspen Technology, Inc., 2014.

[42] H.K: Versteeg and W. Malalasekera. *An Introduction to Computational Fluid Dynamics - The Finite Volume Method*. Longman Scientific & Technical, 1995. ISBN 0-470-23515-2.

[43] Salim M Salim and S C Cheah. Wall y + Strategy for Dealing with Wall-bounded Turbulent Flows. *International MultiConference of Engineers and Computer Scientists (IMECS)*, II:1–6, 2009. doi: 10.1.1.149.722.

[44] Donald E Spiel. On the births of film drops from bubbles bursting on seawater surfaces smaller than their parents and which have upward velocity oscillation. 103 (Cll):907–918, 1998.

[45] Aijun Guo, Xuejun Zhang, and Zongxian Wang. Simulated delayed coking characteristics of petroleum residues and fractions by thermogravimetry. *Fuel Processing Technology*, 89(7):643–650, jul 2008. ISSN 03783820. doi: 10.1016/j.fuproc.2007.12.006.

[46] I E Kuzora, V A Yushinov, and S G Krashchuk. Preparation of Feedstock for Delayed Coking Unit. *Chemistry and Technology of Fuels and Oils*, 36(3):44–46, 2000.

[47] D F Varfolomeev and A I Stekhun. Processing heavy crudes by delayed coking. *Chemistry and Technology of Fuels and Oils*, (7):8–10, 1985.

[48] A I Yushinov, I E Kuzora, V A Krivykh, and S G Krashchuk. Experience in operating a delayed coking unit. *Chemistry and Technology of Fuels and Oils*, 36(3):41–43, 2000.

[49] Lida Tian, Benxian Shen, and Jichang Liu. Building and Application of Delayed Coking Structure-Oriented Lumping Model. 2012.

[50] J A D Mun, R Aguilar, L C Castan, and J Ancheyta. Comparison of Correlations for Estimating Product Yields from Delayed Coking. *Energy and Fuels*, 2013.

[51] Ashish N Sawarkar, Aniruddha B Pandit, Shriniwas D Samant, and Jyeshtharaj B Joshi. Petroleum Residue Upgrading Via Delayed Coking : A Review. *The Canadian Journal of Chemical Engineering*, 85:1–24, 2007.

[52] M L Yang, J Long, C Fan, and W M Zhong. Petroleum Science and Technology Industrial delayed coking process optimization on the basis of lumped kinetic model Industrial delayed coking process optimization on the basis of lumped kinetic model. *PETROLEUM SCIENCE AND TECHNOLOGY*, 34:888 – 902, 2016. doi: 10.1080/10916466.2016.1172088.

[53] A L Chvertkin. Experience in startup and shakedown of delayed coking units. *Chemistry and Technology of Fuels and Oils*, (5):5–7, 1983.

[54] Norman P. Lieberman. *Troubleshooting Process Operations*. PennWell Corporation, Tulsa, Oklahoma, 4th ed. edition, 2009. ISBN 0071180826.

[55] Coby W. Stewart, Aaron M. Stryk, and Lee Presley. Coke drum design. *Petroleum Technology Quarterly*, 11(4):63–69, 2006. ISSN 1362363X.

[56] Sergio Salazar, Rafael Urbina, and Alejandra Meza. Evaluation of potential improvements in the quality of the venezuelan delayed doke through management of the conditions of design and operation of the drum of coking. 35(2):4–9, 2015.

[57] John Reynolds. API risk-based inspection project update, 1997.

[58] Amit V. Mahulkar, Geraldine J. Heynderickx, and Guy B. Marin. Simulation of coking in convection section of steam cracker. *Chemical Engineering Transactions*, 29:1375–1380, 2012. ISSN 19749791. doi: 10.3303/CET1229230.

[59] Jim Roth and Harry Janssen. Coke Drum Outlet Overhead Deflector Plate Aparatus and Method. 1(19), 2002.